

Towards a robust out-of-the-box neural network model for genomic data

Zhaoyi Zhang*

Songyang Cheng*

*Department of Computer Science
University of Wisconsin-Madison
Madison, WI 53715, USA*

ZZHANG825@WISC.EDU

SCHENG72@WISC.EDU

Claudia Solís-Lemus[†]

*Wisconsin Institute for Discovery
and Department of Plant Pathology
University of Wisconsin-Madison
Madison, WI 53715, USA*

SOLISLEMUS@WISC.EDU

Abstract

The accurate prediction of biological features from genomic data is paramount for precision medicine and sustainable agriculture. For decades, neural network models have been widely popular in fields like computer vision, astrophysics and targeted marketing given their prediction accuracy and their robust performance under big data settings. Yet neural network models have not made a successful transition into the medical and biological world due to the ubiquitous characteristics of biological data such as modest sample sizes, sparsity, and extreme heterogeneity.

Here, we investigate the robustness, generalization potential and prediction accuracy of widely used convolutional neural network and natural language processing models with a variety of heterogeneous genomic datasets. Mainly, recurrent neural network models outperform convolutional neural network models in terms of prediction accuracy, overfitting and transferability across datasets. While the perspective of a robust out-of-the-box neural network model is out of reach, we identify certain model characteristics that translate well across datasets and could serve as a baseline model for translational researchers.

Keywords: Generalization error, phenotype prediction, convolutional, natural language processing

Background

The ability to accurately predict phenotypes from genomic data is one of the most coveted goals of modern-day medicine and biology. Examples abound: from precision medicine where researchers want to predict a patient’s disease susceptibility based on the genetic information (Ashley, 2015; Rost et al., 2016; Katuwal and Chen, 2016; Krittanawong et al., 2017; Lee et al., 2018; Ho et al., 2019) to prediction of antibiotic-resistant bacterial strains based on the genomes of pathogenic microbes (Fjell et al., 2009; Coelho et al., 2013; Pesesky

*. Joint first authors with equal contribution and randomly chosen order (reproducible script in Supplementary Material)

†. Corresponding author

et al., 2016; Kavvas et al., 2018; Li et al., 2018). Examples extend beyond human health into soil and plant health such as the prediction of crops yield (or plant disease susceptibility) based on soil microbiome metagenomic data (Chang et al., 2017; Bokulich et al., 2018; Carrieri et al., 2019) and the prediction of pesticide-resistant microbial strains from plant bacterial pathogen genomes (Yang and Guo, 2017; Ip et al., 2018; Maino et al., 2018; Duarte-Carvajalino et al., 2018). Our ability to anticipate outcomes from data is at our scientific core when we face human disease, environmental challenges, and climate change.

Naturally, biologists and medical researchers have turned to the machine-learning community for answers given the great success of machine-learning methods in a plethora of applications such as computer vision (Hjelmås and Low, 2001; Egmont-Petersen et al., 2002) and astrophysics (Kucuk et al., 2017; Jonas et al., 2018) to name a few.

However, the success of machine-learning methods on other fields has not been easily translated to the biological realm (Chen et al., 2019; Ekins et al., 2019; Teschendorff, 2019; Dacrema et al., 2019). Indeed, the complexity of biological omics data has hampered the adoption of machine-learning models, especially neural networks. Among the main challenges of genomic data in neural network models are 1) smaller sample sizes compared to other fields, 2) highly imbalanced datasets, and 3) heterogeneity of training samples and testing samples.

First, despite the advance in high-throughput sequencing technologies, extracting whole genomes remains a time-consuming and expensive task when sample sizes must be in the order of thousands. In addition, data privacy and restrictions on data sharing in medical research restrict scientists' ability to combine multiple smaller datasets into larger ones suitable for neural network modeling.

Second, more important than sample size, the weak link of deep learning in biological applications is the assumption of homogeneity between training and testing samples. This assumption is violated, for example, in microbial datasets where laboratory samples (training data) and environmentally or clinically collected samples (testing data) can be intricately heterogeneous. This data heterogeneity can cause lack of robustness and generalization errors in neural network models. Robustness is the key ingredient that is needed for neural network models to translate into medical practice and into the phenotype prediction in the agricultural or environmental field.

In literature, there are multiple examples of successfully fit neural network models on biological or medical genomic data (Andrew and DeLong, 2015; Zhou and Troyanskaya, 2015; Kelley et al., 2016; Nguyen et al., 2016; Zeng et al., 2016; Agarwal et al., 2019; Trabelsi et al., 2019; Shadab et al., 2020). However, it remains uncertain whether the proposed models could be translated to other similar datasets with comparable performance. That is, we ask whether the neural network models proposed in literature are robust across heterogeneous (but similar in nature) datasets.

In addition, we approach the existing neural network models with the mindset of a biological or medical user. A biological researcher would see the neural network model in an existing publication and then would try to apply a similar model to their own dataset. First, we explore how easy it is to replicate the analysis on existing publications. Second, by making incremental changes to the model characteristics, we gauge the effect of each model component on the overall performance.

We learn mainly three things: 1) in multiple instances, we are not able to replicate the performance in existing publications either because data is not available, code is not available, or code is corrupted, incomplete or not well-documented; 2) most of the times the good performance of existing models does not translate to alternative datasets, yet we do encounter some model characteristics that are generally robust across datasets and that could serve as a potential baseline model – albeit with modest performance – to start the prediction process from a user perspective, and 3) we find that accurate prediction is a balancing game between underfitting and overfitting, and that small changes in the architecture can have unpredictable outcomes.

The quest for robust neural network models that could tackle the complexities of biological data (and its intrinsic heterogeneity) is imminent. Neural network models cannot be fully applicable in informed patient care, medical or agricultural framework if they cannot guarantee some level of generalization potential given that genomic data are not static but constantly evolving. The difficulty of the prediction problem in biology or medicine is such that it would be naive to believe that there will exist an out-of-the-box model that will be fully transferable (recall the “No Free Lunch” (NFL) theorem (Wolpert and Macready, 1997): improved performance over one class of problems is offset by performance over another class). Yet, from a user perspective, it is desirable to know if there are certain model characteristics that perform modestly under scrutiny from a variety of different datasets.

While we advise biological or medical users against using out-of-the-box strategies, we conclude from our study that recurrent neural networks are relatively robust across genomics datasets and generally not affected by the size or type of the data. Overfitting is an issue on more complex CNN models (as expected), but it is relatively controlled via regularization schemes. We also found that a general LSTM layer for embedding performed relatively well across datasets and outperforms more intuitive data encoding schemes like doc2vec which performs poorly on all the scenarios we tested. Finally, our work raises awareness to the importance of reproducibility and replicability. As machine-learning scientists, it is crucial to accompany our work with reproducible scripts that are relatively easy to follow by the scientific community so that our findings have an impact across fields, in particular, into the biological and medical community.

Methods

We focus on convolutional neural networks (CNN) (Zeng et al., 2016; Nguyen et al., 2016; Shadab et al., 2020; Trabelsi et al., 2019) and natural language processing (NLP) (Le and Mikolov, 2014; Agarwal et al., 2019; Dutta et al., 2018) on three datasets of increasing size from the available ones in the papers under study (Table 1) and described below.

SPLICE DATA.

In (Nguyen et al., 2016), the authors included a splice dataset (also in the UCI machine learning repository (Dua and Graff, 2017)). Splice junctions are points on a DNA sequence at which superfluous DNA is removed during the process of protein creation in higher organisms. This dataset has 3190 sequences of length 60 bp and are classified into three classes: exon/intron boundaries (EI: 24%), intron/exon boundaries (IE: 24%), and non-splice (N: 52%).

HISTONE DATA.

In (Nguyen et al., 2016), the authors included 10 datasets about DNA sequences wrapping around histone proteins. We focus on the H3 occupancy from the histone dataset that has 14,965 sequences of length 500 bp. The H3 indicates the histone type, and the dataset has two classes: the positive class includes DNA sequences that contain regions wrapping around histone proteins (51%) and the negative class does not (49%).

MOTIF DISCOVERY DATA.

In (Zeng et al., 2016), the authors included two ChIP-seq datasets: motif discovery and motif occupancy. These datasets contain the labels of the binding affinity of transcription factors to DNA sequence in 690 different ChIP-seq experiments. We only focus on a subset of 269,100 sequences from the motif discovery data (out of 20,464,149) of length 101. The dataset contains two classes: positive class includes DNA sequences that are motif (50%) and negative class includes DNA sequences that are not motif (50%).

DATA SPLITTING.

For all CNN models, we use the following split of the data. The splice dataset is split into 75% for training and 25% for testing with 15% of training data used for validation. The histone dataset is split into 70% for training, 15% for validation, and 15% for testing. The motif discovery data is split into 48.7% for training, 2.6% for validation, and 48.7% for testing. We note that the data partition for the motif discovery dataset deviates from the standard 70-15-15 or 75-25 data partitions. The rationale for this data partition is that the motif discovery data was stored in 690 different files each with a different number of sequences. Given that we do not know how these datasets were created, we wanted to have a uniform representation from all datasets in the training process. The smallest file had 190 sequences, so we randomly selected 190 sequences for each of the 690 files to be used in training. This represents 48.7% of samples used for training. A higher proportion of training samples would imply that some files would be over-represented which could introduce unintended biases in prediction. We choose the same proportion for testing to be able to evaluate the model better given the high heterogeneity of the data leaving only 2.6% for validation.

We note that data encoding differs for the CNN models and the NLP models, so we describe the encoding procedure in the next sections for each type of model.

Convolutional Neural Networks

We test the performance of four convolutional neural network (CNN) models found in literature (Zeng et al., 2016; Nguyen et al., 2016; Shadab et al., 2020; Trabelsi et al., 2019) that have been successful on genomic-based prediction. We assess their performance on their own datasets (when available) and on alternative similar datasets, as well as under incremental modifications of the model characteristics such as data encoding, window size and number of layers. See Table 2 for a summary of the performance tests and models. For all models, we use the cross-entropy loss.

CNN-NGUYEN MODEL (NGUYEN ET AL., 2016).

We implement the simple neural network in (Nguyen et al., 2016) as our baseline model (Figure 1). The model contains two 2D convolutional layers, each followed by a pooling layer, then the output of the convolutional layers are connected to a fully connected layers. The fully connected layer has a dropout rate of 0.5 to reduce the effect of overfitting. Finally, we use a softmax layer to predict the labels of the input sequences. We denote this original model as CNN-Nguyen2D in the results. In addition to this model, we construct a new model with an extra 1D convolutional layer denoted CNN-Nguyen2D+1D for performance comparison. We compare the performance of the model with a different dimension (1D) and increasing number of layers (Figure 2). For splice and histone datasets, the batch size is 32 and for motif discovery dataset, the batch size is 512. Kernel size is (3, 3) for all 2D convolutional layers and (1, 3) for the 1D layer in CNN-Nguyen2D+1D. The number of filters in convolutional layer doubles each time we add a new set of these layers (e.g. 16 filters in the first convolutional layer, 32 in the second, 64 in the third). We use the Adam optimizer with learning rate 0.001 and train for 50 epochs which was assessed to allow sufficient training time for convergence (lack of change in loss over the last few epochs) on all datasets. Early Stopping Callback is not used when training these models as convergence was easily assessed in these cases by studying the loss dynamics.

CNN-ZENG MODEL (ZENG ET AL., 2016).

We implement the neural network model in (Zeng et al., 2016) (Figure 3) that contains two 2D convolutional layers each followed by a batch-normalization and max-pooling layer. The output of the convolutional layers is connected to a fully connected layer. This layer has a dropout rate of 0.5 to prevent overfitting. Finally, a softmax layer is used to predict the class of the input sequence. We denote the original model as CNN-Zeng2 in the results because it has two 2D convolutional layers. We create two new model extensions: CNN-Zeng3 and CNN-Zeng4 with three and four 2D convolutional layers respectively. To explore the effect of the number of layers, we add 2D convolutional, batch-normalization, and max-pooling layers to the end of the convolutional network (Figure 3). For splice and histone datasets, the batch size is 32 and for motif discovery dataset, the batch size is 512. Kernel size is (3, 3) for all 2D convolutional layers. The number of filters in convolutional layer doubles each time we add a new set of these layers (e.g. 16 filters in the first convolutional layer, 32 in the second, 64 in the third). We use the Adam optimizer with learning rate 0.001 and train for 50 epochs which was assessed to allow sufficient training time for convergence (lack of change in loss over the last few epochs) on all datasets. Early Stopping Callback is not used when training these models as convergence was easily assessed in these cases by studying the loss dynamics.

DEEPDBP MODEL (SHADAB ET AL., 2020).

Even though the source code of this paper is not well structured and contains many different models that are not properly documented, we implemented a model based on the paper description which is what a domain practitioner (like a biomedical researcher) would do. The model architecture contains an embedding layer, a convolutional layer, max-pooling layer, followed by fully connected layers and the output layer (Figure 4). For splice and

histone datasets, the batch size is 32 and for motif discovery dataset, the batch size is 512. Kernel size is (1, 3) for the 1D convolutional layer with 128 filters. We use the Adam optimizer with learning rate 0.001 and train for 50 epochs which was assessed to allow sufficient training time for convergence (lack of change in loss over the last few epochs) on all datasets. Early Stopping Callback is not used when training these models as convergence was easily assessed in these cases by studying the loss dynamics. Unlike CNN-Nguyen, CNN-Zeng and DeepRAM which only have one dropout layer at the dense layer, the DeepDBP model has three dropout layers: dropout – dense – dropout – dense – dropout – dense (output) with dropout rate of 0.3.

DEEPRAM MODEL (TRABELSI ET AL., 2019).

We implement the three models in (Trabelsi et al., 2019): 1D convolutional neural networks (Figure 5) denoted DeepRAM-CNN, recurrent neural networks (Figure 6) denoted DeepRAM-RNN, and a mixture of 1D convolutional and recurrent neural networks (Figure 7) denoted DeepRAM-CNN-RNN. For convolutional neural networks, we use two 1D convolutional layers, with each followed by a max-pooling layer, and finally fully connected layer (with a dropout rate of 0.5 to prevent overfitting) and output layer. For splice and histone datasets, the batch size is 32 and for motif discovery dataset, the batch size is 512. Kernel size is (1, 3) for the 1D convolutional layer. The number of filters in convolutional layer doubles each time we add a new set of these layers (e.g. 16 filters in the first convolutional layer, 32 in the second). We use the Adam optimizer with learning rate 0.001 and train for 50 epochs which was assessed to allow sufficient training time for convergence (lack of change in loss over the last few epochs) on all datasets. Early Stopping Callback is not used when training these models as convergence was easily assessed in these cases by studying the loss dynamics. For recurrent neural networks, we use two Long Short-Term Memory (LSTM) layers followed by fully connected layers and output layer. For the hybrid neural networks, we use two 1D convolutional layers and two Long short-term memory layers, and finally fully connected layers and output layers. We note that the DeepRAM-RNN and the DeepRAM-CNN-RNN models are not entirely CNN models and share many characteristics with the Natural Language Processing (NLP) models we will describe next. However, we present these models in this section given that they are all part of the DeepRAM paper (Trabelsi et al., 2019) and we follow the comparisons and analyses highlighted in this work. We compare the changes in performance based on the data encoding as well as comparing the performance of convolutional vs recurrent models.

DATA ENCODING.

For the first three models (CNN-Nguyen, CNN-Zeng and DeepDBP), we use the same data encoding as in (Nguyen et al., 2016). A sliding window of fixed size k allows us to traverse the sequence focusing on windows of length k . The window of length k is a sequence of k nucleotides denoted k -mer. The slide stride is how many nucleotides the window moves to the right as it is traversing the sequence. At each step, a k -mer is read from the sequence and added to the k -mer sequence. For example, if a sequence looks like “ACTGG”, a window size of 3 with slide stride of 1 would produce the 3-mers [“ACT”, “CTG”, “TGG”]. The process is similar to how n -grams are created from text with the k -mer being the word

and k being the “word size”. After that, one-hot encoding is applied to the k -mers. To also include to spatial information of the sequences, we concatenate the encoding of k -mers within a fixed region size. For example, for the 3-mers [“ACT”, “CTG”, “TGG”], a region of 2 would imply that we concatenate [“ACT”, “CTG”] to build the 2D encoded data matrix (see Figure 4 in (Nguyen et al., 2016) for more details). As in (Nguyen et al., 2016), we choose a window size of 3 with slide stride of 1 and a region of 2.

For the DeepRAM models, we experiment with two different ways of encoding the sequences. One way is, as described before, to use one-hot encoding with word size 3 and region size 2. The other way is to convert sequences into overlapping k -mers, and embed k -mers into dense vectors using embedding layers. Note that this embedding is different from the one used in the NLP models (described in next section) because of the unit used for encoding. Here, we use the k -mer as the unit for encoding while in NLP models described next, we use the nucleotide as the unit.

Natural Language Processing in conjunction with Neural Networks Models for Prediction

Traditionally, genomic data is stored as a collection of long strings comprised of the four nucleotides: A,C,G,T. It is thus intuitive to turn to Natural Language Processing (NLP) theory for solid ways to embed the sequences in a latent space. Furthermore, NLP methods naturally overcome one of the main drawbacks of CNN models which is the sparsity of the input vectors.

Here, we focus on two widely used NLP tools: doc2vec (Le and Mikolov, 2014; Kimothi et al., 2016) and Long Short Term Memory (LSTM) (Hochreiter and Schmidhuber, 1997; Agarwal et al., 2019; Kimothi et al., 2016). Both methods share the same objective: represent the input sequence with a low dimensional dense vector yet the specifics differ as is explained below.

We first clarify that the NLP methods are not performing prediction (as the CNN models). Since the purpose of this work is to compare the performance of neural network models on the prediction of phenotypes from genomes, we need to add a neural network model to the NLP model that will perform the prediction of labels (Figure 11). Table 3 presents a summary of the performance tests and models. For all NN models, we use the cross-entropy loss.

LSTM-LAYER MODEL.

We implement the neural network model (Figure 8) that contains, after the input layer, an embedding layer followed by an LSTM layer with size of 30 for both datasets. There are four dense layers with size decaying by a factor of 2 (128-64-32-16). There is one dropout layer between any two dense layers with dropout rate of 0.2. With this model, we study the changes in performance when using different optimizers: Adam and SGD. For the Adam optimizer, we use a learning rate of 0.001 and for SGD optimizer, we used a learning rate of 0.01. We use Early Stopping Callback on both Adam and SGD optimizers with a maximum number of epochs set at 4000 for the splice and the histone data, and 200 for the motif discovery data. The patience parameter (the threshold to stop the training if the loss stops decreasing further after a certain number of epochs) is set at 100 for both

optimizers for the splice data, at 100 and 400 for Adam and SGD respectively for the histone data, and at 10 for both optimizers for the motif discovery data. Changes in the patience parameter are due to differences in speed between the two optimizers when training. For the splice data, training with the Adam optimizer stopped early at 289 epochs while training with SGD optimizer stopped early at 2872 epochs. For the histone data, training with the Adam optimizer stopped early at 154 epochs and at 526 for the SGD optimizer. Finally, for the motif discovery data, training stopped early at 51 epochs for the Adam optimizer, but training reached the maximum number of epochs allowed (200) for the SGD optimizer bringing into question the convergence of such training.

DOC2VEC+NN MODEL (LE AND MIKOLOV, 2014; KIMOTHI ET AL., 2016).

The nature of the doc2vec sequence representation as a semantic vector preserves similarity of sequences in terms of frequency and location of n-grams. We apply the distributed memory mode (DV-PM) as in (Le and Mikolov, 2014; Kimothi et al., 2016), and then, we use the simple fully connected neural network in Figure 11 containing two dense layer with size shrinking by a factor of 2 with a dropout layer in between. We study the effect of embedding size in the performance of the model. For all instances of this model, we use the SGD optimizer with learning rate of 0.01 and momentum of 0.9. We use Early Stopping Callback with maximum number of iterations allowed as 1000 for the splice and histone data, and 400 for the motif discovery data. The patience parameter is set at 50 for the splice data, 30 for the histone data and 10 for the motif discovery data. Again, changes in the maximum number of iterations and patience parameter are due to the speed of training for different sample sizes. Training stopped early on all instances of the model. For the splice data, training stopped early at 119, 143, 166, and 264 epochs for the four embedding sizes used (50, 100, 150, and 200). For the histone data, training stopped early at 114, 177, 61, and 118 for the four embedding sizes used (50, 100, 150, and 200). For the motif discovery data, training stopped early at 36, 39, 58, and 11 for the four embedding sizes used (50, 100, 150, and 200).

LSTM-AE+NN MODEL (AGARWAL ET AL., 2019).

A LSTM autoencoder model (LSTM-AE) aims to represent a sequence by a dense vector that can be converted back to the original sequence. Indeed, LSTM-AE is comprised of two parts: an encoder network (Figure 9) that compresses the original sequence into a low dimensional dense vector, and a decoder network (Figure 10) that converts the vector back to the original sequence. The encoder reads as input an encoded DNA sequence and outputs a dense vector as the embedding for this sequence whose length is a hyper parameter to tune. The decoder reads as input the dense vector produced by the encoder and produces a reconstructed sequence. The accuracy of the autoencoder is measured by comparing the reconstructed sequence to the original sequence. We implement a LSTM-AE following (Agarwal et al., 2019) based on the description in their publication given that no reproducible script was available. The LSTM-AE model is trained to achieve maximum reconstruction accuracy of the sequences. Then, since LSTM-AE is not performing classification, we add a simple fully connected neural network (Figure 11) containing two dense layer with size shrinking by a factor of 2 with a dropout layer in between for the prediction

of class labels. The size of the first dense layer is adjusted, as a rule of thumb, to match 1 to 4 times the embedding dimension. We denote this model as LSTM-AE+NN. We note that only the weights corresponding to the simple fully connected neural network are optimized for classification which is different to the LSTM-layer model whose embedding indeed changes during training. We highlight that the LSTM-layer and LSTM-AE models differ on how an embedding is evaluated. The embedding produced by the LSTM-layer model aims to better classify the sequences into the right category while the embedding produced by the LSTM-AE model aims to better capture the sequence itself. We study the effect of the batch size in the performance of the model. For the LSTM-AE training, we use the Adam optimizer with learning rate of 0.001 while for the training of the simple NN for prediction, we use the SGD optimizer with momentum of 0.9 and with learning rate of 0.01 for the splice and motif discovery data, and 0.001 for the histone data. We use Early Stopping Callback on all cases with 2000, 4000 and 200 maximum iterations allowed for splice, histone and motif discovery data respectively for the LSTM-AE training, and 1000, 1500 and 500 maximum iterations allowed for splice, histone and motif discovery data respectively for the simple NN training. In terms of the patience parameter, we set it at 100, 200 and 10 for the splice, histone and motif discovery data respectively for both LSTM-AE and simple NN training. The LSTM-AE training stopped early in almost all cases: 1) for the splice data, at epoch 1474, 424, and 1005 for the three batch sizes used (32, 256, and 1024 respectively); for the histone data, at epoch 549, 422, and 646 for the three batch sizes used (32, 256, and 1024 respectively), and 3) for the motif discovery data, at epoch 78 and 195 for batch sizes 32 and 256. For this data, training reached the maximum number of iterations allowed (200) for the case of batch size of 1024 bringing into question the convergence of this case. The training of the simple NN stopped early in all cases: 1) for the splice data, at epoch 123, 114, and 200 for the three batch sizes used (32, 256, and 1024 respectively); for the histone data, at epoch 212, 805, and 999 for the three batch sizes used (32, 256, and 1024 respectively), and 3) for the motif discovery data, at epoch 185, 146, and 62 for the three batch sizes used (32, 256, and 1024 respectively).

We summarize the training details for the NLP models in Table 4. We note that since the training of the CNN was simpler (50 epochs in all cases), we do not need a summarizing table for the training of the CNN models.

DATA ENCODING.

For the LSTM-layer and the LSTM-AE models, we use the same data encoding. Each nucleotide is converted to a label number. For example, [“A”, “C”, “G”, “T”], are encoded as [3, 2, 1, 0] in descending lexicographical order. The LSTM-layer is crucial given the intractable growth in dimension of the input vector. That is, a sequence containing 6000 nucleotides would be represented by a sequence of 6000 numbers. For the doc2vec model, we encode the sequences based on 3-mers with slide stride of 1. For example, for the “ACTGG” sequence, the 3-mers are [“ACT”, “CTG”, “TGG”]. We construct a dictionary with all the 3-mers in the training set. While it is unlikely for 3-mers in the test set to not appear in the dictionary, we categorize these instances as out-of-vocabulary (OOV) with a unique encoding.

Results

The role of dimension and number of layers on CNN

Figure 12 shows the training, validating and testing accuracy of the CNN models when varying the number of layers for the three datasets. Nguyen2D corresponds to the original CNN model in (Nguyen et al., 2016), while Nguyen2D+1D corresponds to the same model with an extra 1D convolutional layer. Similarly, Zeng2 corresponds to the original model in (Zeng et al., 2016) which has two 2D convolutional layers while Zeng3 and Zeng4 correspond to models with three and four 2D convolutional layers respectively.

For the smallest dataset (splice), all models have a testing accuracy higher than 80% which is similar to what is reported in the original CNN-Nguyen paper (Nguyen et al., 2016) (88.9%) except for the original model in CNN-Zeng (Zeng et al., 2016) (denoted Zeng2 because it has two layers). Adding more layers improves the performance of the CNN-Zeng model, but not the CNN-Nguyen model. There is not any strong evidence of overfitting in any of the models in the splice data.

For the medium size dataset (histone), all models have a similar testing accuracy (slightly below 80%). In this dataset, adding more layers merely increases the training accuracy and thus, the overfitting. Lastly, for the largest dataset (motif discovery), all testing accuracies are below 70%. There is a slight improvement in the CNN-Nguyen model when adding one more 1D layer, yet for the case of CNN-Zeng, more layers only increase the training accuracy and thus, the overfitting. We compare the performance of the CNN-Zeng model with and without regularization in the Appendix.

To sum up, accuracy decreases with data size with the largest data having the lowest reported accuracy. In addition, adding more layers to a CNN model does increase accuracy for smaller datasets, but it appears to only increase overfitting on larger datasets. This assertion is counterintuitive as overfitting is thought to be the result of parameter-rich models on small size data. In our analyses, overfitting indeed appears as a result of more complex models (more layers) yet only on larger datasets. It is important to note that this atypical performance could be due to the distinct data partition chosen for the motif discovery data (48-3-48 in contrast to a standard 70-15-15). For this dataset, we prioritized a equal contribution to the training samples from each of the 690 input files in order to prevent unintended bias in predictions caused by heterogeneity in the sequences. This choice is not meant to be perfect and can create another set of complications (e.g., the unexpected decreased accuracy). Future work should address implications in prediction due to data partition choices when faced with highly heterogeneous datasets.

We investigate the precision-recall curves of the models in Figure 13. The CNN-Nguyen models outperform those in CNN-Zeng across datasets with the original CNN-Zeng2 displaying the worse performance. This behavior is confirmed with the ROC curves in Figure 14.

The role of data encoding

It appears that the type of data encoding (one-hot encoding vs embedding layer) does not have a strong influence on the performance of the DeepRAM models in (Trabelsi et al., 2019). Figure 15 shows the accuracy of the models which is lowest overall for the largest

dataset (motif discovery) yet there is not a clear difference across models or data encoding types. The combined model (CNN-RNN) seems to slightly outperform the other models and this behavior is also apparent in the precision-recall curves (Figure 16) and in the ROC curves (Figure 17). However, care must be taken in that the combined model with embedding layer (CNN-RNN-Embed) seems to overfit in the motif discovery data while the one-hot encoding version of the same model does not show overfitting, so it appears that one-hot encoding should be preferred.

Importantly, the behavior of DeepRAM seems to translate well across datasets. Accuracy lies between 80% and 90% for the smallest dataset (splice) and around 75% for the largest dataset (motif discovery). As a point of comparison, the accuracy presented in original DeepRAM paper (Trabelsi et al., 2019) ranges from 83.6% to 99.4% on data from 83 ChIP-seq experiments in the ENCODE project.

The role of the optimizer

The SGD optimizer outperforms the Adam optimizer on the LSTM-layer model for the smallest dataset (splice) while Adam outperforms SGD for the two larger datasets (histone and motif discovery). See Figure 18 for accuracy, Figure 19 for precision-recall curves and Figure 20 for ROC curves. While (Reddi et al., 2019) has already discussed the convergence issues of the Adam optimizer, we also need to note that the difference in performance can be due to differences with the Early Stopping Callback patience parameter. It is widely accepted that SGD performs better in terms of finding global optima. However, due to its low speed, it can get stuck in one plateau too long. We note that the comparison of optimizer behavior has ignited multiple studies. For a more comprehensive investigation on the role of optimizers in neural network models, see (Nado et al., 2021).

The role of the embedding size

Of all the neural network models compared in this work, the doc2vec version performs the worse with accuracy barely exceeding 50% (Figure 21). The size of embedding does not appear to have a strong influence on the accuracy, and if anything, it appears to slightly decrease accuracy as the size of embedding increases for some datasets (e.g. histone). The poor performance of the doc2vec models is evident in the precision-recall curves (Appendix) and the ROC curves as well (Appendix). This behavior contradicts the results of the original work of doc2vec on sequences (Kimothi et al., 2016) which reported 97% specificity (true negative rate), 93% sensitivity (true positive rate or recall), and 95% accuracy for binary classification (as in histone and motif discovery data) and 83% precision, 81.5% sensitivity, 81% accuracy for multiclass classification (as in splice data). The lack of congruence could be due to lack of robustness of the model across datasets, but more likely can be explained by the length of the sequences. While the original study has an average length of 425 bp with sequences as long as 22,152 bp, the sequences used here have length 60, 101 and 500.

The role of batch size

Batch size has zero impact on the accuracy of the LSTM-AE model (Agarwal et al., 2019) (Figure 22) with all three batch sizes (32, 256 and 1024) showing the same accuracy levels

for a given dataset. Accuracy is instead affected by the size of the data with the largest dataset (motif discovery) barely exceeding 50%. Also, this model appears to be robust to overfitting across datasets. The same conclusions can be drawn from the precision-recall curves (Figure 23) and the ROC curves (Figure 24). In the precision-recall curve it stands out that the class 0 in the splice data is harder to be predicted with his model compared to the other classes.

Overall comparison of models

Among of all options, we select the models with highest testing accuracy for each of the categories (listed in Table 5): CNN-Nguyen (Nguyen et al., 2016), CNN-Zeng (Zeng et al., 2016), DeepRAM (Trabelsi et al., 2019), doc2vec, LSTM-AE (Agarwal et al., 2019) and LSTM-layer and for each of the three datasets (splice, histone and motif discovery). We also add the model in DeepDBP (Shadab et al., 2020) to the comparison.

Regarding accuracy (Figure 25), first, we note that the behavior of DeepDBP is not robust across datasets with accuracy levels never exceeding 55% for the histone and motif discovery data while the reported accuracy on the original paper (Shadab et al., 2020) was 84.31% for a data of size 1075. It appears that the performance of DeepDBP is highly dependent on the specifics of the data at hand.

Next, we notice that doc2vec+NN behaves poorly with accuracy levels barely exceeding 50% in all three datasets. We reiterate that this poor performance could be due to the short length of the sequences. Overall, DeepRAM outperforms all other models across datasets which has the added strength of robustness given that the accuracy levels are not far from the accuracy levels reported in the original DeepRAM paper (Trabelsi et al., 2019) (88.9%). Both CNN models (Nguyen and Zeng) perform well across datasets albeit less accurately than DeepRAM. Overfitting does not appear to be a relevant factor among these models, except for CNN-Nguyen on the histone data.

Figure 26 shows the precision-recall curves where the same conclusions are confirmed with DeepRAM outperforming all models in the histone and motif discovery datasets. The CNN models (Nguyen and Zeng) outperform all models for the splice data. We note that prediction of class 0 in the splice data appears to be harder than prediction of the other two classes as evidenced by lower overall curves. The doc2vec model performs poorly on all datasets. Similar conclusions are drawn with the ROC curves (Figure 27) with DeepDBP behaving as a random predictor on the histone and motif discovery data.

Discussion

Neural network models provide endless opportunities for prediction and classification in biological applications (Peng et al., 2020; Alber et al., 2019), yet much remains unknown regarding the transferability of the performance across datasets. Robustness across datasets of similar nature is a key ingredient to translate neural network models into medical, agricultural or environmental practice. Here, we study the performance on genomic data of convolutional neural networks (CNN) and neural network models assisted by natural language processing (NLP). We highlight that the conclusions we found are restricted to the datasets and the models selected, and thus, more work is needed to be able to extend conclusions beyond the current study.

We find that DeepRAM outperforms all other models especially the recurrent version (RNN) in terms of prediction accuracy, overfitting, and robustness across datasets. Compared to CNN models (CNN-Nguyen and CNN-Zeng) whose prediction accuracy dramatically decreases with larger datasets, DeepRAM models experience a much smaller accuracy decrease. Furthermore, the accuracy levels of DeepRAM that we find here are comparable to those reported in the original DeepRAM paper (Trabelsi et al., 2019) and thus, we can conclude that the DeepRAM models are more robust, transferable and generalizable across genomic datasets with varied characteristics. It is interesting to notice that DeepRAM outperforms CNN-Nguyen and CNN-Zeng even when we are using the original datasets in both CNN papers (Nguyen et al., 2016; Zeng et al., 2016).

DeepDBP lacks robustness across datasets at least for the datasets compared in this work. The original paper of DeepDBP (Shadab et al., 2020) reported prediction accuracy levels of 84.31% and while we find a prediction accuracy of around 90% for the splice data, for the histone and motif discovery datasets, the DeepDBP prediction accuracy barely exceeds 50%. Furthermore, the DeepDBP paper did not provide usable reproducible scripts that we could follow, so the poor performance could be due to discrepancies between the model implemented here and the model implemented in the original DeepDBP. Given that our goal was to approach this study from the perspective of a domain practitioner (biomedical researcher), we believe that such researcher would read a NN article (like the DeepDBP), and then try to fit such model on their own data. When NN papers provide clear code (python notebooks, for example), they facilitate this task to practitioners. The authors of DeepDBP, however, did not provide clear code to fit their models, so we test the performance of a model based on the paper description (which is what the biomedical researcher would do). We hope to bring attention to reproducibility practices to help domain practitioners fit NN models that appear in literature in their own datasets.

In terms of overfitting, the gap between training and testing accuracy increases as the number of layers increases for CNN models. This behavior is more evident for larger datasets (histone and motif discovery) than smaller datasets (splice). We reiterate that this atypical performance could be due to the choice of data partition into 48.7% training set for the motif discovery data (far from the standard 70-15-15 data partition). While this choice was made in an attempt to reduce bias caused by heterogeneous input sequences, it is far from perfect. Future work should address implications in prediction due to data partition choices when faced with highly heterogeneous datasets.

It is noteworthy that more LSTM layers do not seem to increase overfitting since LSTM-layer (one layer), LSTM-AE (one layer) and DeepRAM-RNN (two layers) have no noticeable overfitting patterns though a more thorough investigation of LSTM layers is still lacking. The only overfitting case for DeepRAM happens on the motif discovery data in the combined model (CNN-RNN) with embedding data encoding. It seems advisable to utilize one-hot encoding for DeepRAM models to prevent the potential of overfitting.

The doc2vec encoding performed poorly on all scenarios. Given that the prediction model for doc2vec and LSTM-AE (Agarwal et al., 2019) is the same (the simple NN in Figure 11) and LSTM-AE dramatically outperforms doc2vec, we do not recommend the use of doc2vec for data embedding and recommend the use of LSTM autoencoders instead. This is especially true for the case of shorter sequences. For the LSTM-AE model, the

batch size made no difference in performance and this model seems to be very robust to overfitting, yet we do see smaller accuracy with larger datasets.

We conclude by raising awareness to the importance of reproducibility in science. In many instances, it was impossible to replicate the results of existing publications given the lack of reproducible well-documented scripts and available data. Reproducibility is crucial not just for the sake of open science, but to maximize the applicability of our machine-learning findings into a biological or medical community who might not have a strong programming background.

Practical advice for domain scientists

Among the models here compared, recurrent neural network models (specifically DeepRAM-RNN (Trabelsi et al., 2019)) outperform convolutional neural network models in terms of prediction accuracy, overfitting and transferability across datasets. More LSTM layers produce higher prediction accuracy without overfitting, unlike more convolutional layers which tend to produce modestly higher accuracy, but also a larger gap between training and testing accuracy. We recommend accompanying extra convolutional layers with regularization. Convolutional neural networks have a reasonable performance overall, but their accuracy is affected by the size of the data with larger (more heterogeneous) datasets having lower prediction accuracy, a behavior not seen with RNN. For data encoding, the intuitive nature of doc2vec does not translate into good prediction performance and less interpretable encoders like LSTM-AE (Agarwal et al., 2019) should be preferred, especially for the case of shorter sequences as illustrated in the three datasets here used. The doc2vec encoder followed by a simple NN performs poorly (accuracy barely exceeding 50%) in all tested scenarios unlike LSTM-AE (Agarwal et al., 2019) followed by the same simple NN which manages moderately good accuracy (comparable to CNN models) across datasets and without too evident overfitting. In terms of model characteristics, embedding size and batch size do not seem to play any important role in our comparisons, and the optimizer does in conjunction with the patience parameter (but see (Nado et al., 2021)).

Appendix

See Figure 28 for the precision-recall plot on the role of the embedding size for the doc2vec model, and see Figure 29 for the ROC curve plot. See Figures 30 and 31 for the effect of regularization on the CNN-Zeng model. Finally, Figures 32 to 36 show the learning dynamics of loss and accuracy for all the models presented in this work.

Reproducible Julia script for random order of first authors

```
using Random
s = 313627913
Random.seed!(s)
people = ["songyang", "zhaoyi"]
people[randperm(length(people))]
```

Acknowledgements

We thank Dr. Aurelie Rakotondrafara and Helena Jaramillo Mesa for the motivation to compare neural network models on plant viral data. We acknowledge the work in (Hotaling, 2020) which helped us improve the scientific writing of this manuscript. We thank the associate editor and the three anonymous reviewers for the insightful comments and suggestions which greatly improved the manuscript.

Funding

This work is supported by the Department of Energy [DE-SC0021016 to CSL].

Availability of data and materials

The data was made publicly available by the original manuscripts. All the scripts developed in this work are publicly available in the GitHub repository <https://github.com/solislemuslab/dna-nn-theory>.

Competing interests

The authors declare that they have no competing interests.

Authors' contributions

ZZ and SC ran all the analyses, researched the literature to find the candidate models to compare, programmed all the open-source code (<https://github.com/solislemuslab/dna-nn-theory>) and wrote an initial draft of the manuscript. CSL developed the idea, created all the plots in the manuscript and wrote the final version of the manuscript.

References

- Vishal Agarwal, N Jayanth Kumar Reddy, and Ashish Anand. Unsupervised representation learning of DNA sequences. *arXiv*, (1906.03087), June 2019.
- Mark Alber, Adrian Buganza Tepole, William R Cannon, Suvranu De, Salvador Duran-Bernal, Krishna Garikipati, George Karniadakis, William W Lytton, Paris Perdikaris, Linda Petzold, et al. Integrating machine learning and multiscale modeling—perspectives, challenges, and opportunities in the biological, biomedical, and behavioral sciences. *NPJ digital medicine*, 2(1):1–11, 2019.
- Babak Alipanahi Andrew and Matthew T DeLong. Weirauch frey brendan j: Predicting the sequence specificities of dna-and rna-binding proteins by deep learning. *Nat Biotechnol*, 10, 2015.
- Euan A Ashley. The precision medicine initiative: a new national effort. *Jama*, 313(21): 2119–2120, 2015.

- Nicholas A Bokulich, Matthew R Dillon, Evan Bolyen, Benjamin D Kaehler, Gavin A Huttenley, and J Gregory Caporaso. q2-sample-classifier: machine-learning tools for microbiome classification and regression. *Journal of open research software*, 3(30), 2018.
- Anna Paola Carrieri, Will PM Rowe, Martyn Winn, and Edward O Pyzer-Knapp. A fast machine learning workflow for rapid phenotype prediction from whole shotgun metagenomes. In *Proceedings of the AAAI Conference on Artificial Intelligence*, volume 33, pages 9434–9439, 2019.
- Hao-Xun Chang, James S Haudenschild, Charles R Bowen, and Glen L Hartman. Metagenome-wide association study and machine learning prediction of bulk soil microbiome and crop productivity. *Frontiers in Microbiology*, 8:519, 2017.
- Po-Hsuan Cameron Chen, Yun Liu, and Lily Peng. How to develop machine learning models for healthcare. *Nature Materials*, 18(5):410–414, 2019.
- Joana Rosado Coelho, João André Carriço, Daniel Knight, Jose-Luis Martínez, Ian Morrissey, Marco Rinaldo Oggioni, and Ana Teresa Freitas. The use of machine learning methodologies to analyse antibiotic and biocide susceptibility in staphylococcus aureus. *PLoS One*, 8(2):e55582, 2013.
- Maurizio Ferrari Dacrema, Paolo Cremonesi, and Dietmar Jannach. Are we really making much progress? a worrying analysis of recent neural recommendation approaches. In *Proceedings of the 13th ACM Conference on Recommender Systems*, RecSys ’19, page 101–109, New York, NY, USA, 2019. Association for Computing Machinery. ISBN 9781450362436. doi: 10.1145/3298689.3347058. URL <https://doi.org/10.1145/3298689.3347058>.
- Dheeru Dua and Casey Graff. UCI machine learning repository, 2017. URL <http://archive.ics.uci.edu/ml>.
- Julio M Duarte-Carvajalino, Diego F Alzate, Andrés A Ramirez, Juan D Santa-Sepulveda, Alexandra E Fajardo-Rojas, and Mauricio Soto-Suárez. Evaluating late blight severity in potato crops using unmanned aerial vehicles and machine learning algorithms. *Remote Sensing*, 10(10):1513, 2018.
- T. Dutta, A. and Dubey, K. K. Singh, and A. Anand. Splicevec: Distributed feature representations for splice junction prediction. *Computational biology and chemistry*, 74: 434–441, 2018.
- Michael Egmont-Petersen, Dick de Ridder, and Heinz Handels. Image processing with neural networks: a review. *Pattern recognition*, 35(10):2279–2301, 2002.
- Sean Ekins, Ana C. Puhl, Kimberley M. Zorn, Thomas R. Lane, Daniel P. Russo, Jennifer J. Klein, Anthony J. Hickey, and Alex M. Clark. Exploiting machine learning for end-to-end drug discovery and development. *Nature Materials*, 18(5):435–441, 2019.

- Christopher D Fjell, Håvard Jenssen, Kai Hilpert, Warren A Cheung, Nelly Pante, Robert EW Hancock, and Artem Cherkasov. Identification of novel antibacterial peptides by chemoinformatics and machine learning. *Journal of medicinal chemistry*, 52(7):2006–2015, 2009.
- Erik Hjelmås and Boon Kee Low. Face detection: A survey. *Computer vision and image understanding*, 83(3):236–274, 2001.
- Daniel Sik Wai Ho, William Schierding, Melissa Wake, Richard Saffery, and Justin O’Sullivan. Machine learning snp based prediction for precision medicine. *Frontiers in Genetics*, 10:267, 2019.
- Sepp Hochreiter and Jürgen Schmidhuber. Long short-term memory. *Neural Comput.*, 9(8):1735–1780, November 1997. ISSN 0899-7667. doi: 10.1162/neco.1997.9.8.1735. URL <https://doi.org/10.1162/neco.1997.9.8.1735>.
- Scott Hotaling. Simple rules for concise scientific writing. *Limnology and Oceanography Letters*, 5(6):379–383, 2020. doi: <https://doi.org/10.1002/lol2.10165>. URL <https://aslopubs.onlinelibrary.wiley.com/doi/abs/10.1002/lol2.10165>.
- Ryan HL Ip, Li-Minn Ang, Kah Phooi Seng, JC Broster, and JE Pratley. Big data and machine learning for crop protection. *Computers and Electronics in Agriculture*, 151:376–383, 2018.
- Eric Jonas, Monica Bobra, Vaishaal Shankar, J Todd Hoeksema, and Benjamin Recht. Flare prediction using photospheric and coronal image data. *Solar Physics*, 293(3):48, 2018.
- Gajendra Jung Katuwal and Robert Chen. Machine learning model interpretability for precision medicine. *arXiv preprint arXiv:1610.09045*, 2016.
- Erol S Kavvas, Edward Catoi, Nathan Mih, James T Yurkovich, Yara Seif, Nicholas Dillon, David Heckmann, Amitesh Anand, Laurence Yang, Victor Nizet, et al. Machine learning and structural analysis of mycobacterium tuberculosis pan-genome identifies genetic signatures of antibiotic resistance. *Nature communications*, 9(1):1–9, 2018.
- David R Kelley, Jasper Snoek, and John L Rinn. Basset: learning the regulatory code of the accessible genome with deep convolutional neural networks. *Genome research*, 26(7):990–999, 2016.
- Dhananjay Kimothi, Akshay Soni, Pravesh Biyani, and James M. Hogan. Distributed representations for biological sequence analysis. *arXiv*, (1608.05949), 2016.
- Chayakrit Krittanawong, HongJu Zhang, Zhen Wang, Mehmet Aydar, and Takeshi Kitai. Artificial intelligence in precision cardiovascular medicine. *Journal of the American College of Cardiology*, 69(21):2657–2664, 2017.
- Ahmet Kucuk, Juan M Banda, and Rafal A Angryk. A large-scale solar dynamics observatory image dataset for computer vision applications. *Scientific data*, 4:170096, 2017.

- Quoc Le and Tomas Mikolov. Distributed representations of sentences and documents. In Eric P. Xing and Tony Jebara, editors, *Proceedings of the 31st International Conference on Machine Learning*, volume 32 of *Proceedings of Machine Learning Research*, pages 1188–1196, Beijing, China, 22–24 Jun 2014. PMLR. URL <http://proceedings.mlr.press/v32/le14.html>.
- Su-In Lee, Safiye Celik, Benjamin A Logsdon, Scott M Lundberg, Timothy J Martins, Vivian G Oehler, Elihu H Estey, Chris P Miller, Sylvia Chien, Jin Dai, et al. A machine learning approach to integrate big data for precision medicine in acute myeloid leukemia. *Nature communications*, 9(1):1–13, 2018.
- Li-Guan Li, Xiaole Yin, and Tong Zhang. Tracking antibiotic resistance gene pollution from different sources using machine-learning classification. *Microbiome*, 6(1):1–12, 2018.
- James L Maino, Paul A Umina, and Ary A Hoffmann. Climate contributes to the evolution of pesticide resistance. *Global Ecology and Biogeography*, 27(2):223–232, 2018.
- Zachary Nado, Justin M Gilmer, Christopher J Shallue, Rohan Anil, and George E Dahl. A large batch optimizer reality check: Traditional, generic optimizers suffice across batch sizes. *arXiv preprint arXiv:2102.06356*, 2021.
- Ngoc Giang Nguyen, Vu Anh Tran, Duc Luu Ngo, Dau Phan, Favorisen Rosyking Lumbanraja, Mohammad Reza Faisal, Bahridin Abapihi, Mamoru Kubo, and Kenji Satou. DNA sequence classification by convolutional neural network. *JBiSE*, 09(05):280–286, 2016.
- Grace C. Y. Peng, Mark Alber, Adrian Buganza Tepole, William R. Cannon, Suvranu De, Salvador Dura-Bernal, Krishna Garikipati, George Karniadakis, William W. Lytton, Paris Perdikaris, Linda Petzold, and Ellen Kuhl. Multiscale modeling meets machine learning: What can we learn? *Archives of Computational Methods in Engineering*, 2020.
- Mitchell W Pesesky, Tahir Hussain, Meghan Wallace, Sanket Patel, Saadia Andleeb, Carey-Ann D Burnham, and Gautam Dantas. Evaluation of machine learning and rules-based approaches for predicting antimicrobial resistance profiles in gram-negative bacilli from whole genome sequence data. *Frontiers in microbiology*, 7:1887, 2016.
- Sashank J. Reddi, Satyen Kale, and Sanjiv Kumar. On the convergence of adam and beyond. *arXiv*, (1904.09237), 2019.
- Burkhard Rost, Predrag Radivojac, and Yana Bromberg. Protein function in precision medicine: deep understanding with machine learning. *FEBS letters*, 590(15):2327–2341, 2016.
- S Shadab, M T A Khan, N A Neezi, S Adilina, and others. DeepDBP: Deep neural networks for identification of DNA-binding proteins. *Informatics in Medicine*, 2020.
- Andrew E Teschendorff. Avoiding common pitfalls in machine learning omic data science. *Nature Materials*, 18(5):422–427, 2019.

Ameni Trabelsi, Mohamed Chaabane, and Asa Ben-Hur. Comprehensive evaluation of deep learning architectures for prediction of DNA/RNA sequence binding specificities. *Bioinformatics*, 35(14):i269–i277, July 2019.

D.H. Wolpert and W.G. Macready. No free lunch theorems for optimization. *IEEE Transactions on Evolutionary Computation*, 1(1):67–82, 1997. doi: 10.1109/4235.585893.

Xin Yang and Tingwei Guo. Machine learning in plant disease research. *European Journal of BioMedical Research*, 3(1):6–9, 2017.

Haoyang Zeng, Matthew D Edwards, Ge Liu, and David K Gifford. Convolutional neural network architectures for predicting DNA-protein binding. *Bioinformatics*, 32(12):i121–i127, June 2016.

Jian Zhou and Olga G Troyanskaya. Predicting effects of noncoding variants with deep learning-based sequence model. *Nature methods*, 12(10):931–934, 2015.

Figures

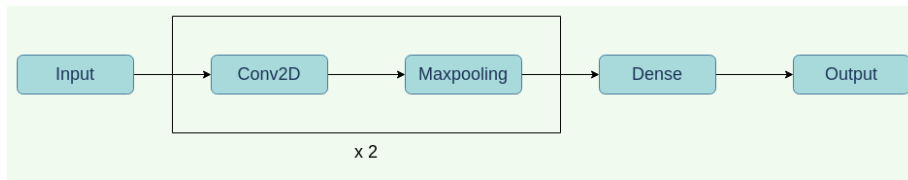


Figure 1: Original CNN-Nguyen (2D) (Nguyen et al., 2016). The dense layer has a dropout rate of 0.5 to prevent overfitting.

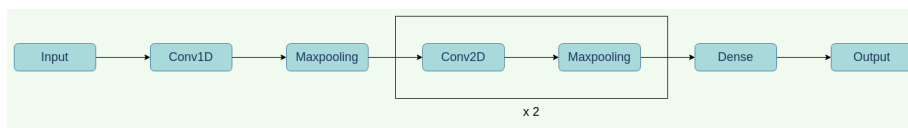


Figure 2: Modified CNN-Nguyen (2D+1D) (Nguyen et al., 2016). The dense layer has a dropout rate of 0.5 to prevent overfitting.

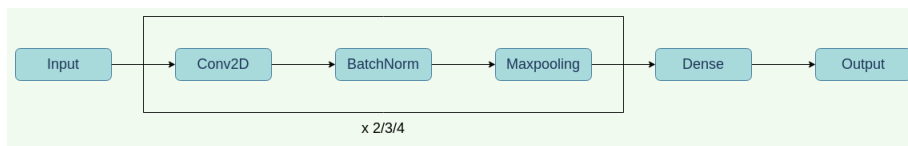


Figure 3: Original CNN-Zeng (2 layers), modified (3,4 layers) (Zeng et al., 2016). The dense layer has a dropout rate of 0.5 to prevent overfitting.

Tables

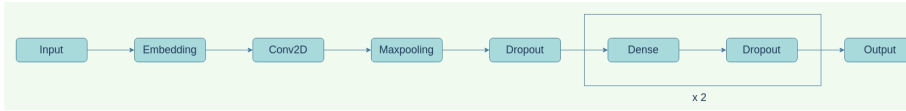


Figure 4: DeepDBP (Shadab et al., 2020)

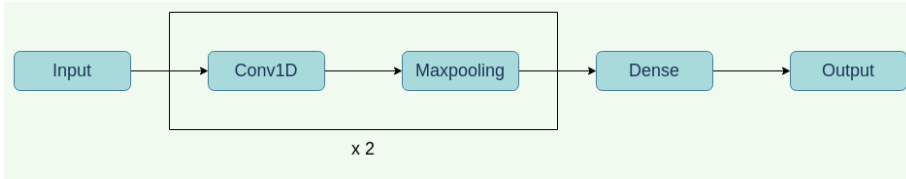


Figure 5: DeepRAM-CNN (Trabelsi et al., 2019). The dense layer has a dropout rate of 0.5 to prevent overfitting.

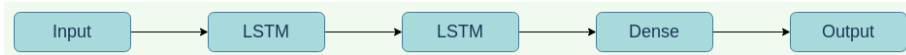


Figure 6: DeepRAM-RNN (Trabelsi et al., 2019). The dense layer has a dropout rate of 0.5 to prevent overfitting.

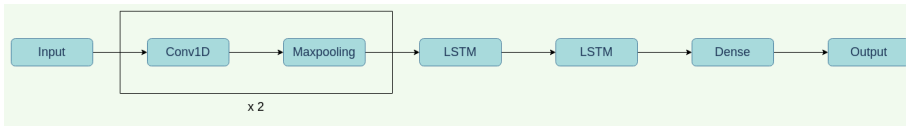


Figure 7: DeepRAM-CNN-RNN (Trabelsi et al., 2019). The dense layer has a dropout rate of 0.5 to prevent overfitting.

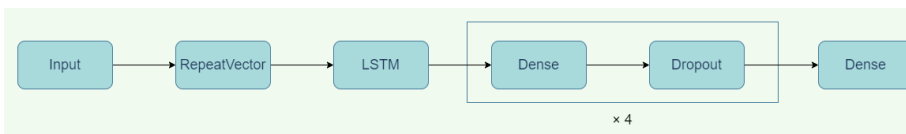


Figure 8: LSTM-layer



Figure 9: LSTM-AE (encoder) (Agarwal et al., 2019)

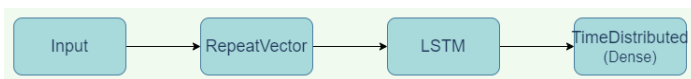


Figure 10: LSTM-AE (decoder) (Agarwal et al., 2019)

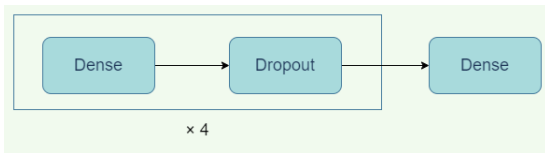


Figure 11: Simple NN for prediction after LSTM-AE (encoder) and doc2vec

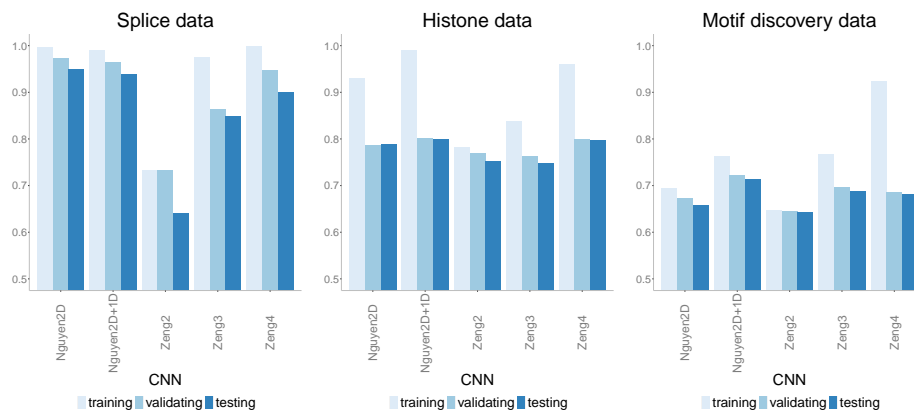


Figure 12: Accuracy of CNN models of increasing number of layers on three datasets of increasing size. Nguyen2D corresponds to the original CNN model in (Nguyen et al., 2016), while Nguyen2D+1D corresponds to the same model with an extra 1D convolutional layer. Similarly, Zeng2 corresponds to the original model in (Zeng et al., 2016) which has two 2D convolutional layers while Zeng3 and Zeng4 correspond to models with three and four 2D convolutional layers respectively. There is an inverse relationship between accuracy and data size with the largest dataset (motif discovery) having the lowest accuracy overall. Adding one layer with different dimension (CNN-Nguyen2D+1D) improves the accuracy slightly, but more layers of the same dimension (CNN-Zeng3 with 3 layers and CNN-Zeng4 with 4 layers) only increase the overfitting.

Table 1: Datasets used to test the neural network models.

Dataset	Sample size	Sequence Length (bp)	Reference
Splice	3190	60	(Nguyen et al., 2016)
Histone	14965	500	(Nguyen et al., 2016)
Motif discovery	269100	101	(Zeng et al., 2016)

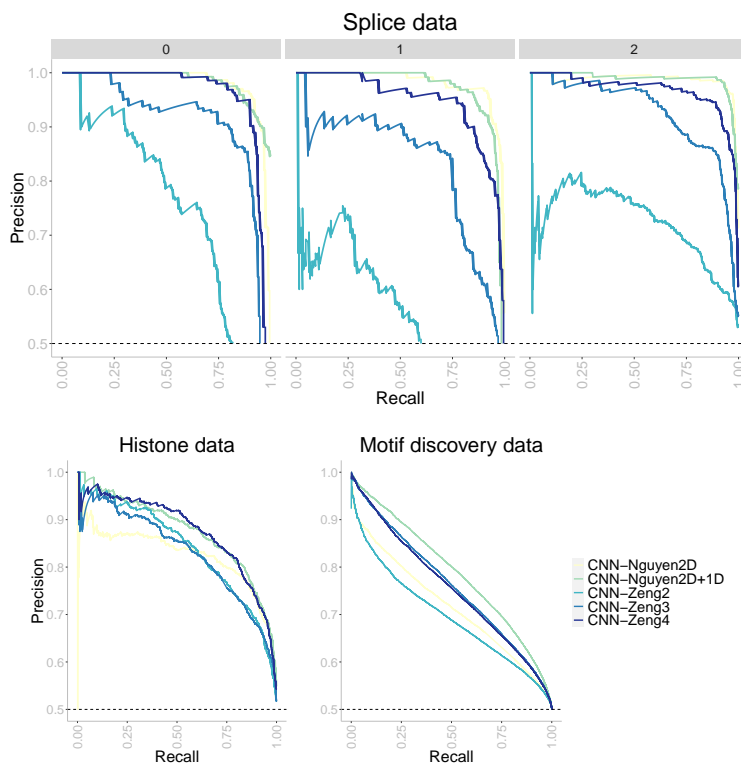


Figure 13: Precision-recall curves of CNN models of increasing number of layers on the three datasets of increasing size. The higher the curve, the better performance with a horizontal dashed line to represent random prediction. An ideal precision-recall curve would cross the (1,1) point. The splice data has three panels since precision-recall curves assume binary classification and the splice dataset has three classes (0, 1, 2). Each panel corresponds to prediction one class vs the other two combined. Nguyen2D corresponds to the original CNN model in (Nguyen et al., 2016), while Nguyen2D+1D corresponds to the same model with an extra 1D convolutional layer. Similarly, Zeng2 corresponds to the original model in (Zeng et al., 2016) which has two 2D convolutional layers while Zeng3 and Zeng4 correspond to models with three and four 2D convolutional layers respectively. The CNN-Nguyen models outperform the other models across datasets.

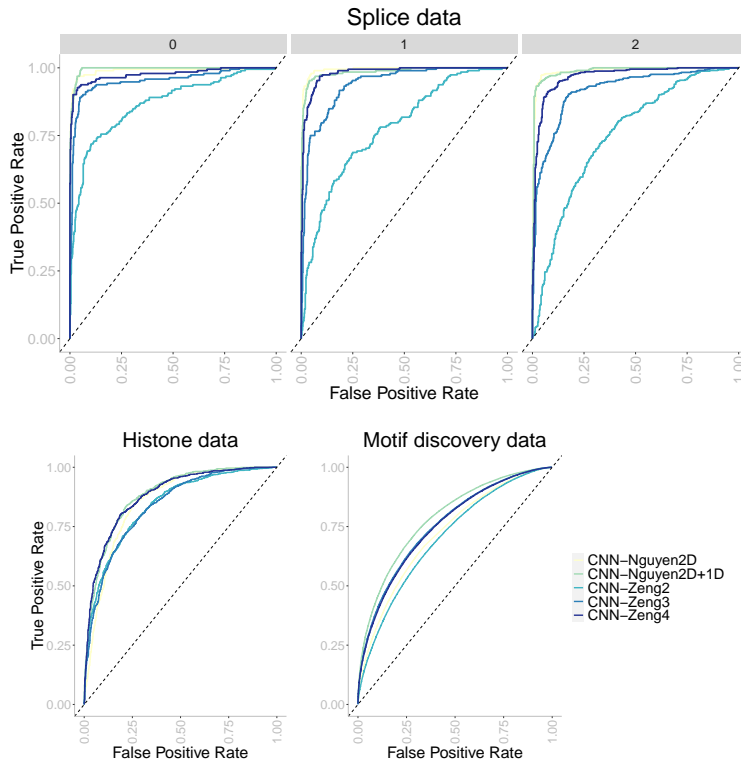


Figure 14: ROC curves of CNN models of increasing number of layers on the three datasets of increasing size. The higher the curve, the better performance with a 45° dashed line to represent random prediction. The splice data has three panels since ROC curves assume binary classification and the splice dataset has three classes (0, 1, 2). Each panel corresponds to prediction one class vs the other two combined. Nguyen2D corresponds to the original CNN model in (Nguyen et al., 2016), while Nguyen2D+1D corresponds to the same model with an extra 1D convolutional layer. Similarly, Zeng2 corresponds to the original model in (Zeng et al., 2016) which has two 2D convolutional layers while Zeng3 and Zeng4 correspond to models with three and four 2D convolutional layers respectively. The CNN-Nguyen models outperform the other models across datasets.

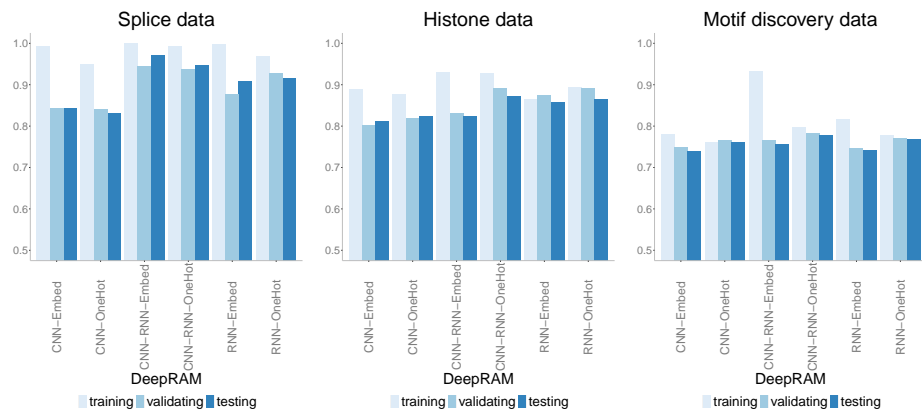


Figure 15: Accuracy of DeepRAM models (Trabelsi et al., 2019) with two different data encoding schemes: one-hot encoding (OneHot) and embedding layer (Embed) on three datasets of increasing size. CNN corresponds to the convolutional model, RNN corresponds to the recurrent model and CNN-RNN corresponds to the combined model. Accuracy decreases with data size, and all models display a similar behavior on the different data encoding schemes.

Table 2: CNN models along with the datasets used and the performance tests

	Model	Own datasets	Outside datasets	Performance tests
CNN-Nguyen (Nguyen et al., 2016)	Figure 1	splice, histone	motif discovery	number of layers, dimension
CNN-Zeng (Zeng et al., 2016)	Figure 3	motif discovery	splice, histone	number of layers
DeepDBP (Shadab et al., 2020)	Figure 4		splice, histone, motif discovery	
DeepRAM (Trabelsi et al., 2019)	Figures 5, 6, 7		splice, histone, motif discovery	data encoding

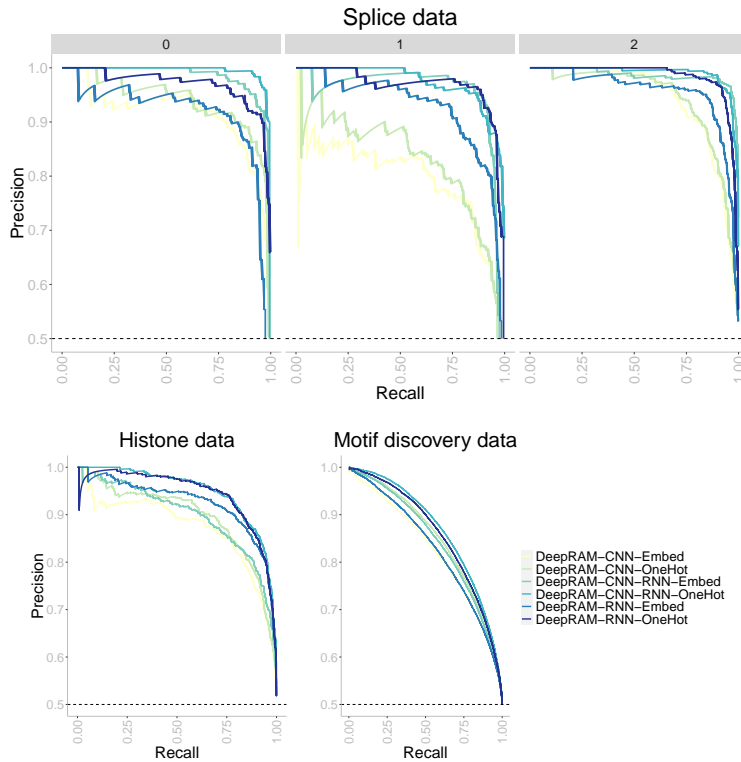


Figure 16: Precision-recall curves of DeepRAM models (Trabelsi et al., 2019) with two different data encoding schemes: one-hot encoding (OneHot) and embedding layer (Embed) on three datasets of increasing size. The higher the curve, the better performance with a horizontal dashed line to represent random prediction. An ideal precision-recall curve would cross the (1,1) point. The splice data has three panels since precision-recall curves assume binary classification and the splice dataset has three classes (0, 1, 2). Each panel corresponds to prediction one class vs the other two combined. CNN corresponds to the convolutional model, RNN corresponds to the recurrent model and CNN-RNN corresponds to the combined model. Accuracy decreases with data size, and all models display a similar behavior on the different data encoding schemes.

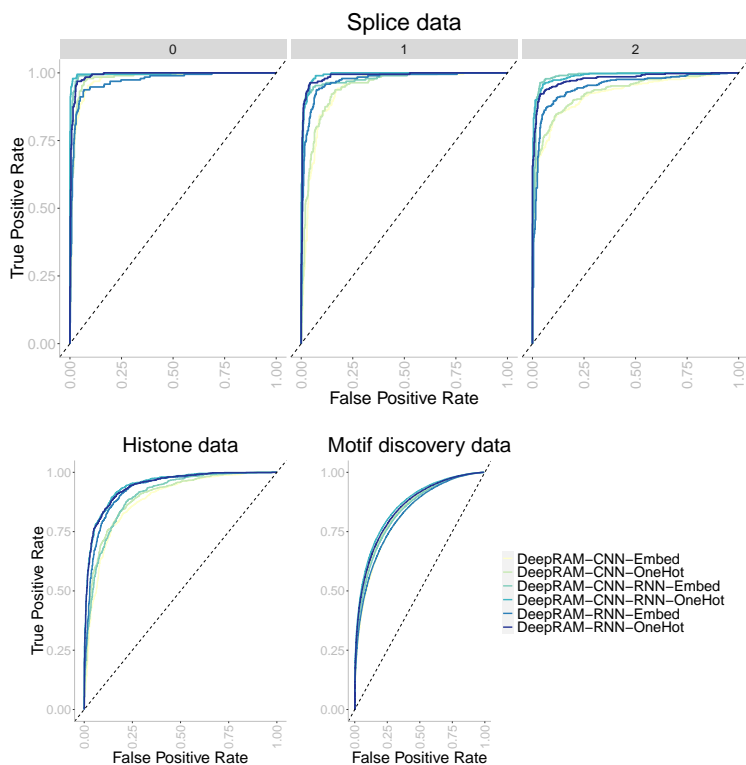


Figure 17: ROC curves of DeepRAM models (Trabelsi et al., 2019) with two different data encoding schemes: one-hot encoding (OneHot) and embedding layer (Embed) on three datasets of increasing size. The higher the curve, the better performance with a 45° dashed line to represent random prediction. The splice data has three panels since ROC curves assume binary classification and the splice dataset has three classes (0, 1, 2). Each panel corresponds to prediction one class vs the other two combined. CNN corresponds to the convolutional model, RNN corresponds to the recurrent model and CNN-RNN corresponds to the combined model. Accuracy decreases with data size, and all models display a similar behavior on the different data encoding schemes.

Table 3: NLP models along with the datasets used and the performance tests

	Model	Own datasets	Outside datasets	Performance tests
LSTM-layer	Figure 8		splice, histone, motif discovery	optimizer
doc2vec+NN (Le and Mikolov, 2014; Kimothi et al., 2016)	Figure 11		splice, histone, motif discovery	embedding size
LSTM-AE+NN (Agarwal et al., 2019)	Figures 9, 11		splice, histone, motif discovery	batch size

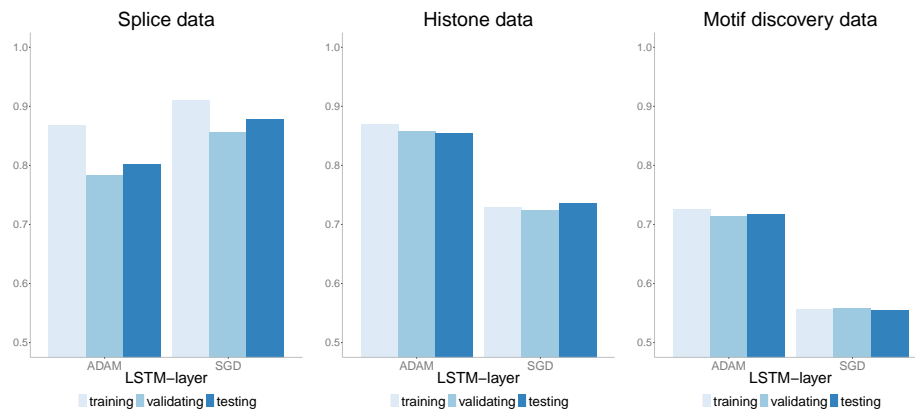


Figure 18: Accuracy of LSTM-layer model with two different optimizers: ADAM and SGD on three datasets of increasing size. There is no evidence of overfitting with this model on any of the datasets. In addition, the best optimizer varies with SGD outperforming ADAM for the smallest dataset (splice) and ADAM outperforming SGD on the other two datasets. It is widely accepted that SGD performs better in terms of finding global optima. However, due to its low speed, it can get stuck in one plateau too long.

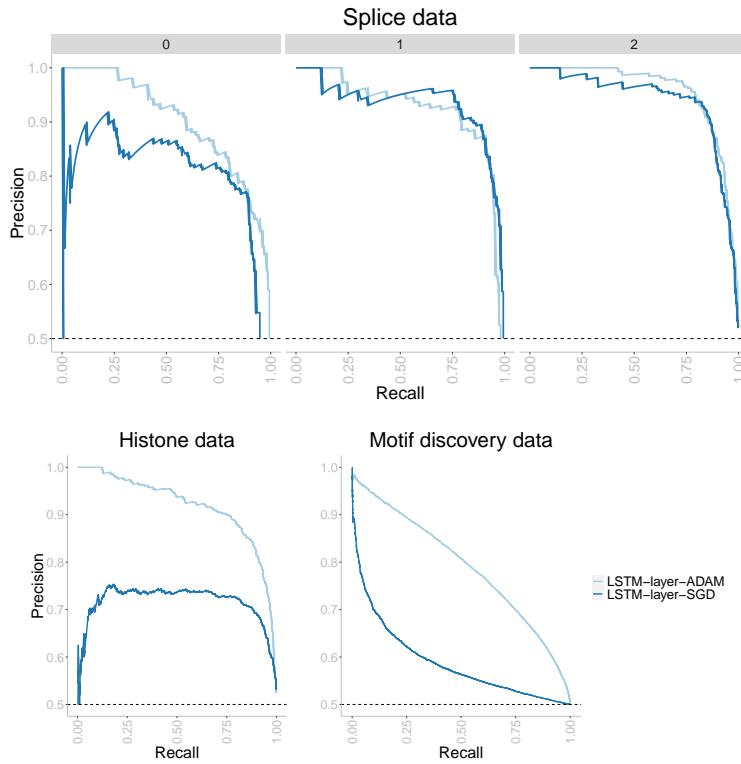


Figure 19: Precision-recall curves of LSTM-layer model with two different optimizers: ADAM and SGD on three datasets of increasing size. The higher the curve, the better performance with a horizontal dashed line to represent random prediction. An ideal precision-recall curve would cross the (1,1) point. The splice data has three panels since precision-recall curves assume binary classification and the splice dataset has three classes (0, 1, 2). Each panel corresponds to prediction one class vs the other two combined. The best optimizer varies with SGD outperforming ADAM for the smallest dataset (splice) and ADAM outperforming SGD on the other two datasets. It is widely accepted that SGD performs better in terms of finding global optima. However, due to its low speed, it can get stuck in one plateau too long.

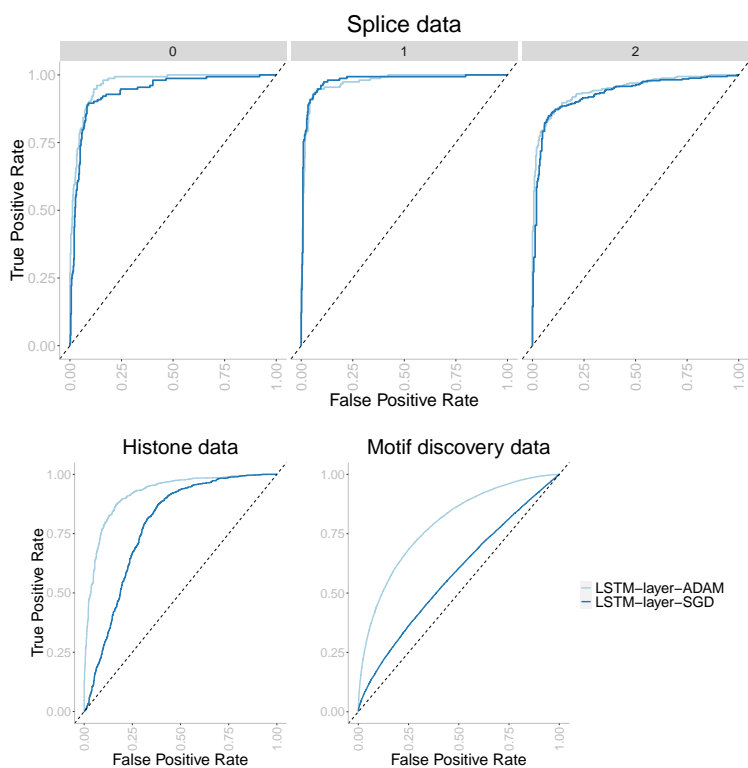


Figure 20: ROC curves of LSTM-layer model with two different optimizers: ADAM and SGD on three datasets of increasing size. The higher the curve, the better performance with a 45° dashed line to represent random prediction. The splice data has three panels since ROC curves assume binary classification and the splice dataset has three classes (0, 1, 2). Each panel corresponds to prediction one class vs the other two combined. The best optimizer varies with SGD outperforming ADAM for the smallest dataset (splice) and ADAM outperforming SGD on the other two datasets. It is widely accepted that SGD performs better in terms of finding global optima. However, due to its low speed, it can get stuck in one plateau too long.

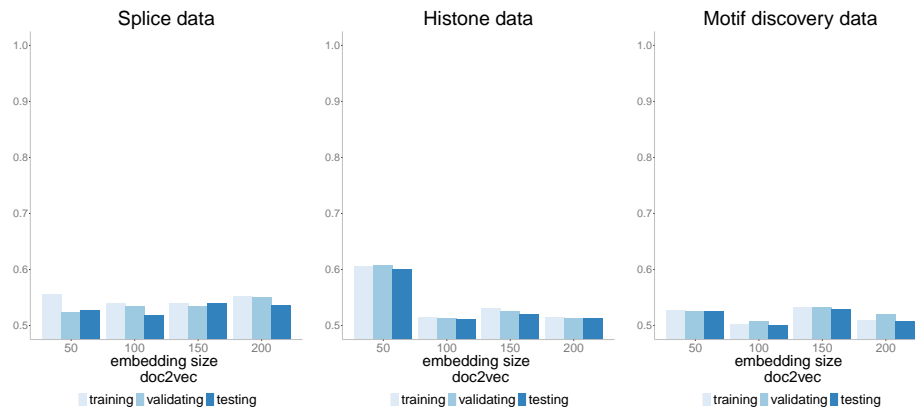


Figure 21: Accuracy of doc2vec+NN model with four different embedding sizes (50, 100, 150, 200) on three datasets of increasing size. The performance is poor in all cases with accuracy barely exceeding 50% across datasets.

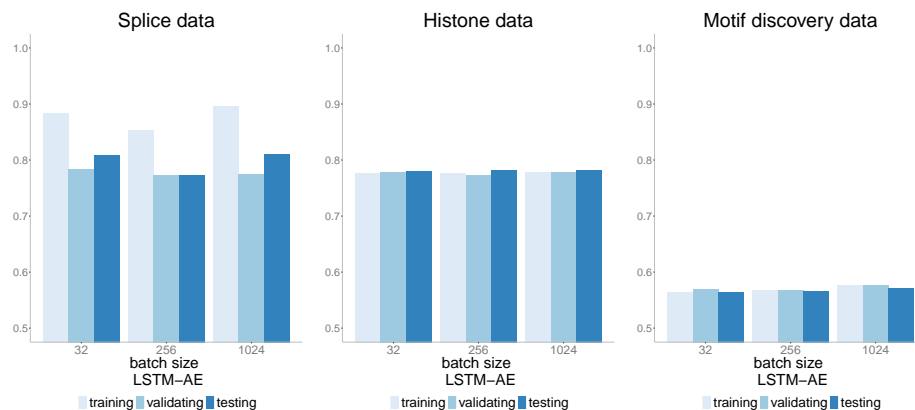


Figure 22: Accuracy of LSTM-AE+NN model (Agarwal et al., 2019) with three different batch sizes (32, 256 and 1024) on three datasets of increasing size. There is no evidence of overfitting with this model, and accuracy seems to decrease as the data size increases with the largest data (motif discovery) having the smallest accuracy (barely above 50%).

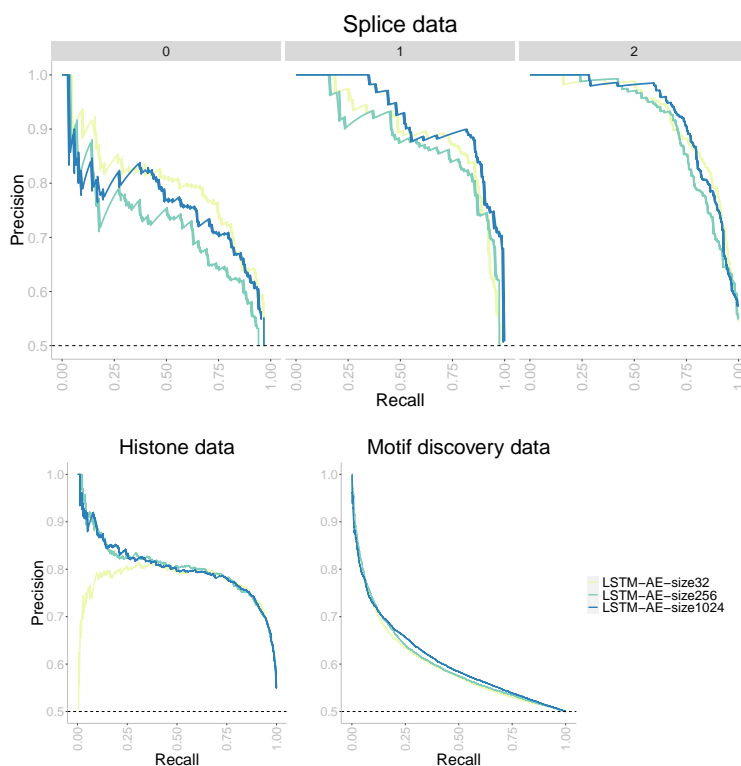


Figure 23: Precision-recall curves of LSTM-AE+NN model (Agarwal et al., 2019) with three different batch sizes (32, 256 and 1024) on three datasets of increasing size. The higher the curve, the better performance with a horizontal dashed line to represent random prediction. An ideal precision-recall curve would cross the (1,1) point. The splice data has three panels since precision-recall curves assume binary classification and the splice dataset has three classes (0, 1, 2). Each panel corresponds to prediction one class vs the other two combined. Unlike other models, there is a clear distinction in the class 0 prediction performance of this model compared to other classes in the splice data. It appears that class 0 is harder to predict with a lower recall for a given precision value compared to the other classes.

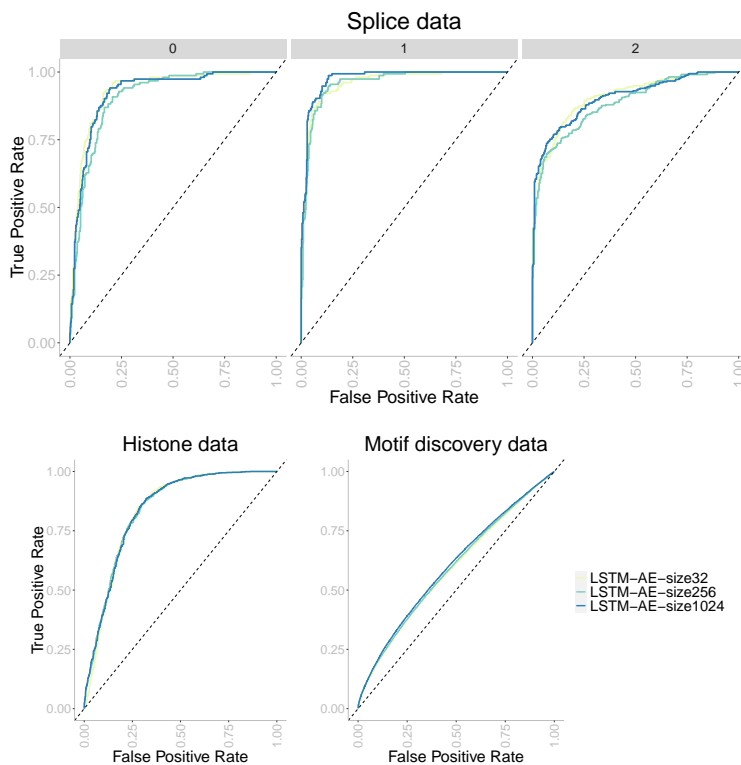


Figure 24: ROC curves of LSTM-AE+NN model (Agarwal et al., 2019) with three different batch sizes (32, 256 and 1024) on three datasets of increasing size. The higher the curve, the better performance with a 45° dashed line to represent random prediction. The splice data has three panels since ROC curves assume binary classification and the splice dataset has three classes (0, 1, 2). Each panel corresponds to prediction one class vs the other two combined. Again, we see no differences with respect to batch size and ROC curves close to the 45° dashed line (random prediction) for the motif discovery data.

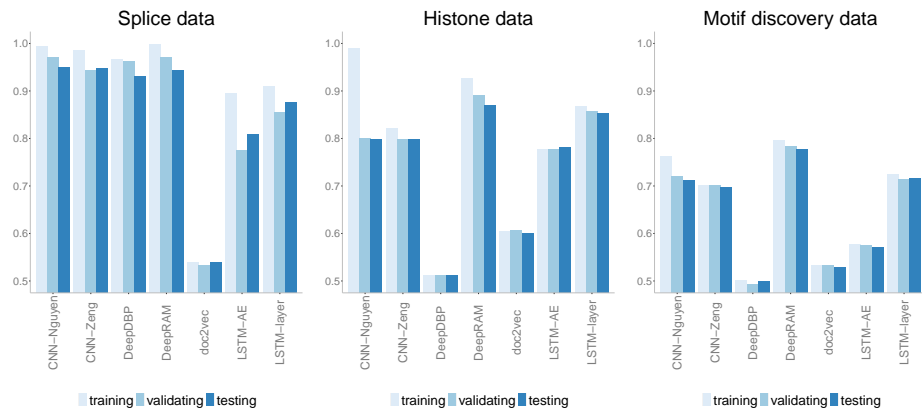


Figure 25: Accuracy of the models with highest testing accuracy among all comparisons (Table 5) across datasets. DeepDBP (Shadab et al., 2020) shows the worst robustness across datasets, while DeepRAM (Trabelsi et al., 2019) shows both the best accuracy and robustness across datasets. Overfitting does not appear to be an issue except for CNN-Nguyen on the histone data.

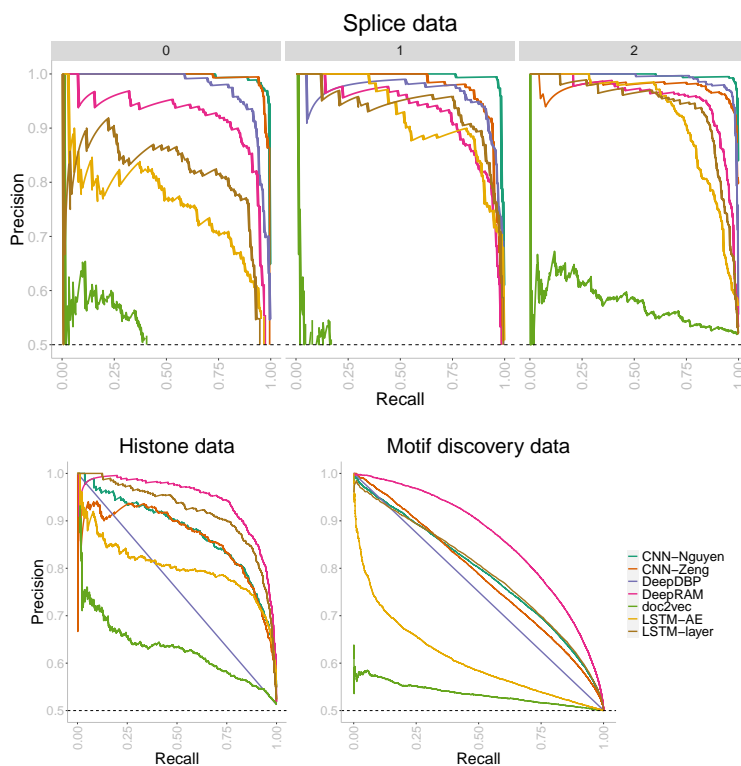


Figure 26: Precision-recall curves of CNN models of increasing number of layers on the three datasets of increasing size. The higher the curve, the better performance with a horizontal dashed line to represent random prediction. An ideal precision-recall curve would cross the (1,1) point. The splice data has three panels since precision-recall curves assume binary classification and the splice dataset has three classes (0, 1, 2). Each panel corresponds to prediction one class vs the other two combined. DeepRAM outperforms all models in the histone and motif discovery datasets, and behaves well on the splice data. The CNN models (Nguyen and Zeng) outperform all models on the splice data.

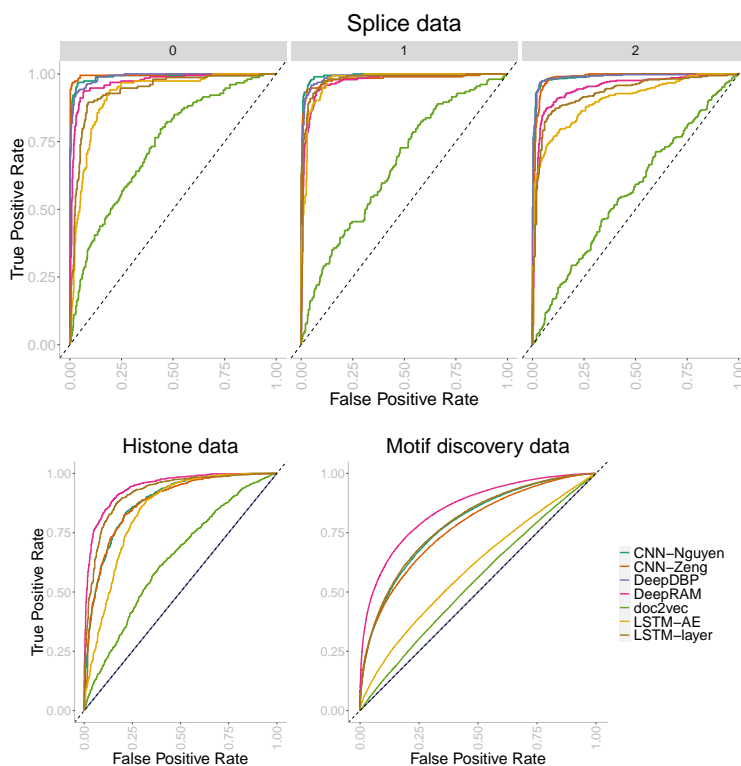


Figure 27: ROC curves of CNN models of increasing number of layers on the three datasets of increasing size. The higher the curve, the better performance with a 45° dashed line to represent random prediction. The splice data has three panels since ROC curves assume binary classification and the splice dataset has three classes (0, 1, 2). Each panel corresponds to prediction one class vs the other two combined. DeepRAM outperforms all models in the histone and motif discovery datasets, and behaves well on the splice data. The CNN models (Nguyen and Zeng) outperform all models on the splice data. DeepDBP behaves as a random predictor on the histone and motif discovery data.

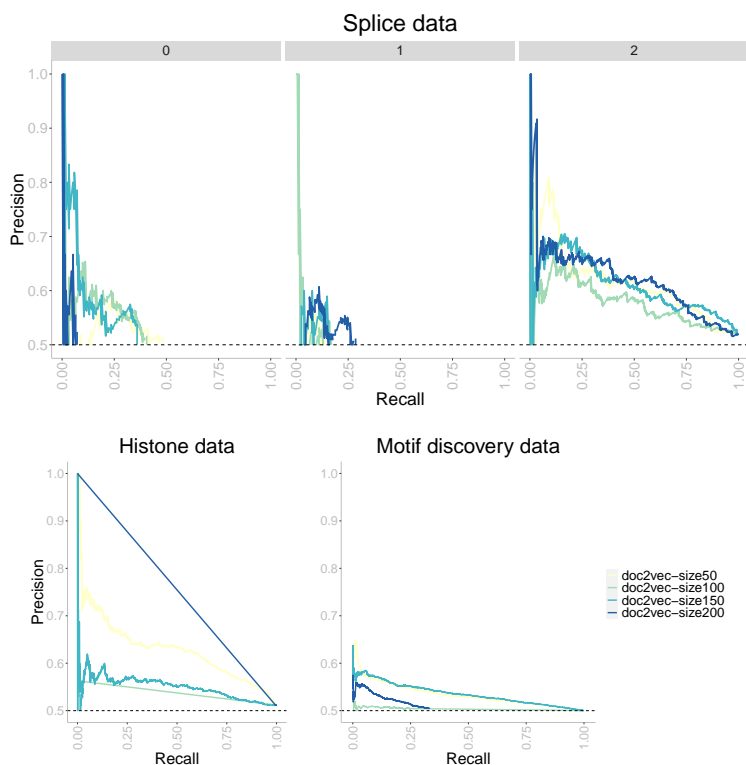


Figure 28: Precision-recall curves of doc2vec+NN model with four different embedding sizes (50, 100, 150, 200) on three datasets of increasing size. The higher the curve, the better performance with a horizontal dashed line to represent random prediction. An ideal precision-recall curve would cross the (1,1) point. The splice data has three panels since precision-recall curves assume binary classification and the splice dataset has three classes (0, 1, 2). Each panel corresponds to prediction one class vs the other two combined. The performance is poor in all cases.

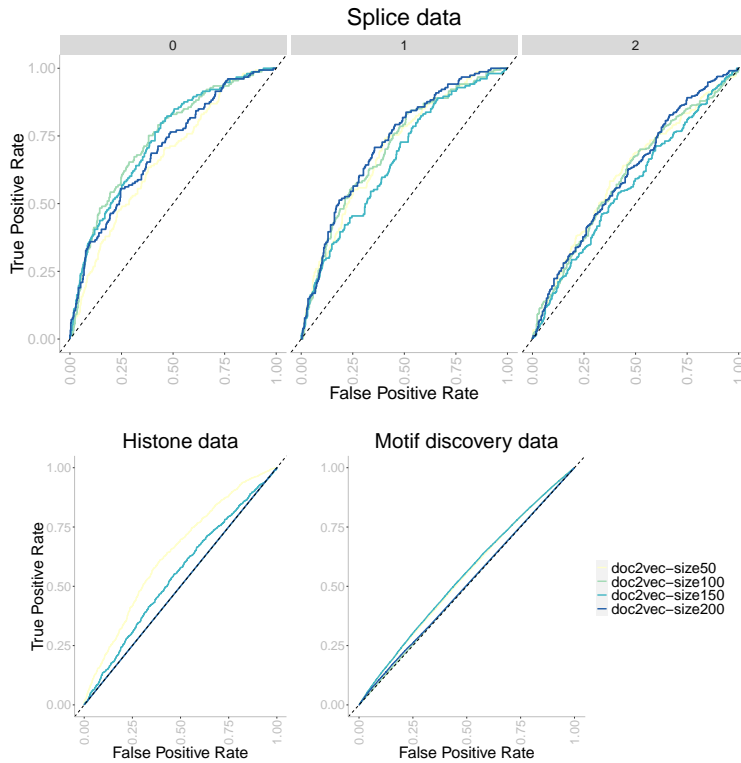


Figure 29: ROC curves of doc2vec+NN model with four different embedding sizes (50, 100, 150, 200) on three datasets of increasing size. The higher the curve, the better performance with a 45° dashed line to represent random prediction. The splice data has three panels since ROC curves assume binary classification and the splice dataset has three classes (0, 1, 2). Each panel corresponds to prediction one class vs the other two combined. The performance is poor in all cases.

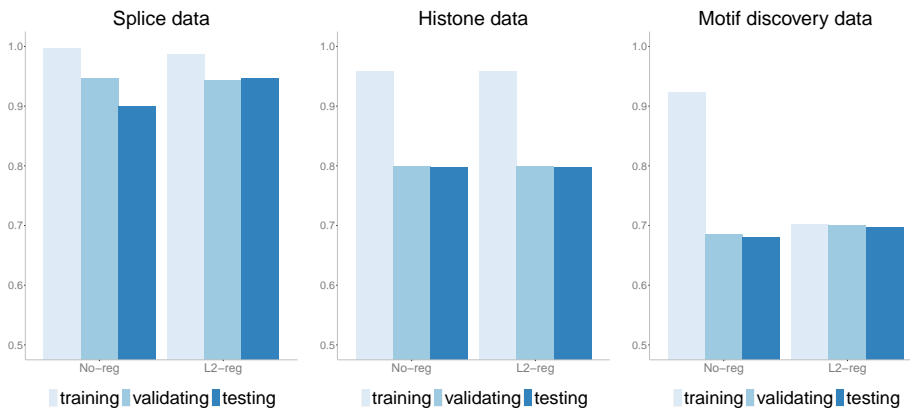


Figure 30: Accuracy of CNN-Zeng models with four 2D layer on three datasets of increasing size with and without regularization. The L2 regularization indeed reduces overfitting for the motif discovery data, but not for the histone data.

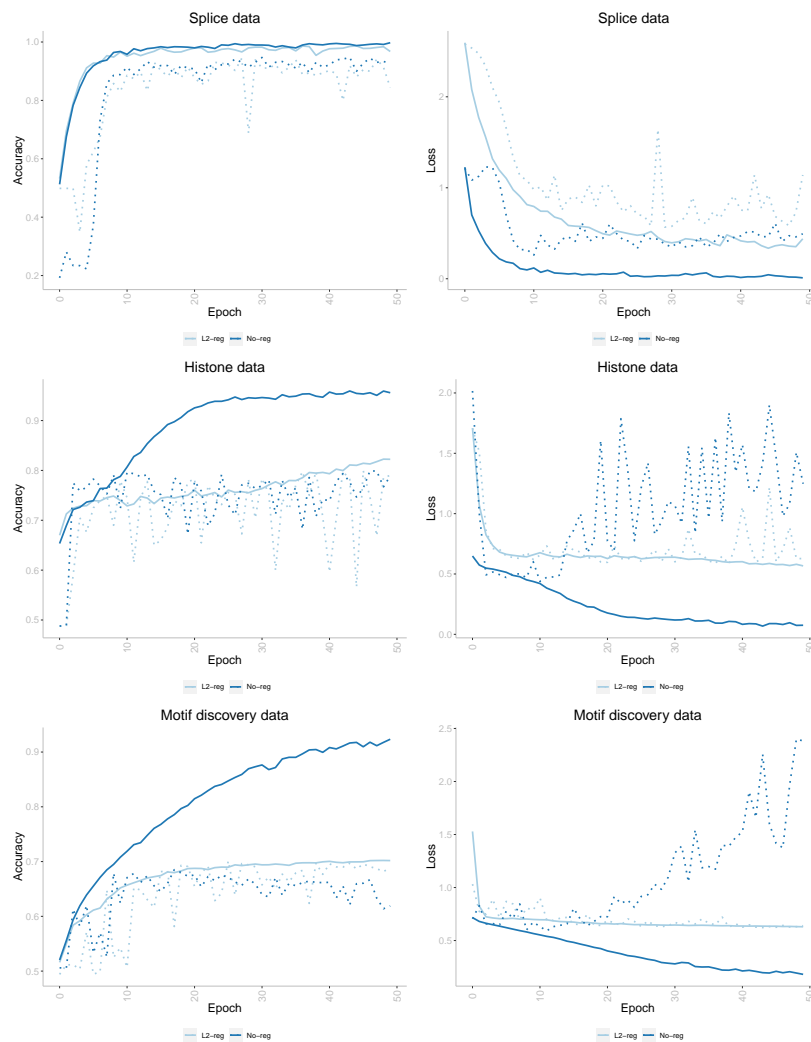


Figure 31: Learning dynamics for CNN-Zeng models with four 2D layer on three datasets of increasing size with and without regularization. Solid lines correspond to training accuracy/loss and dashed lines correspond to validating accuracy/loss. Colors represent no regularization or L2 regularization.

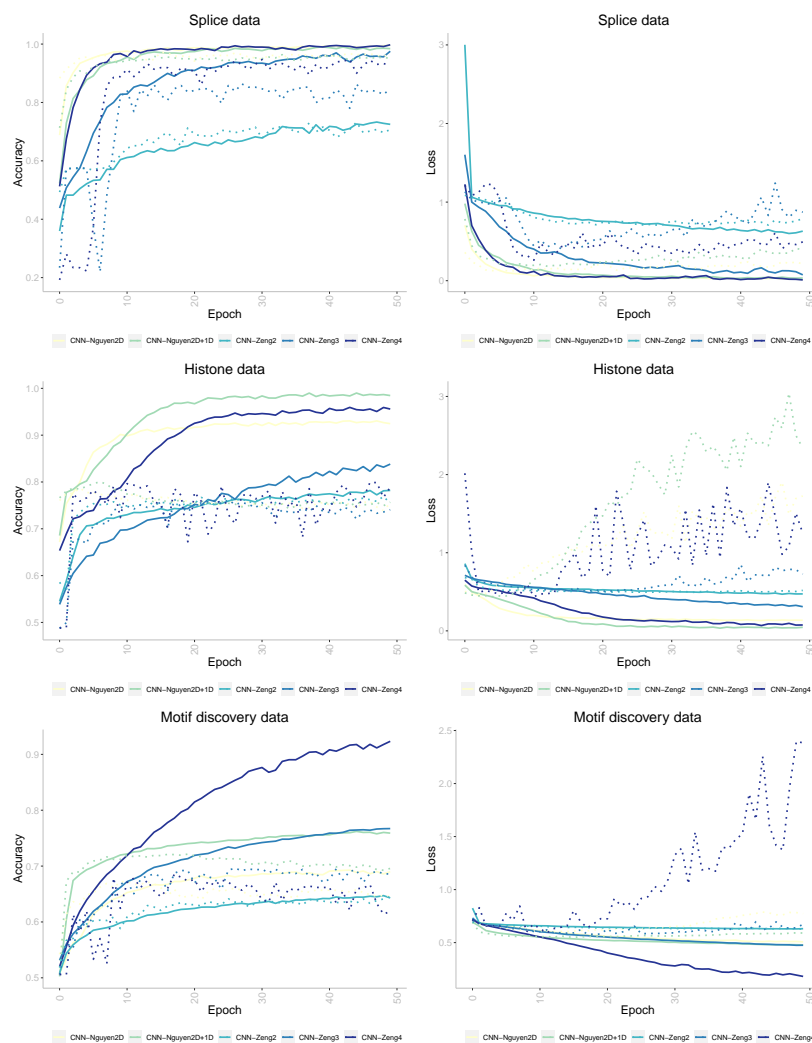


Figure 32: Learning dynamics for CNN models on different datasets. Solid lines correspond to training accuracy/loss and dashed lines correspond to validating accuracy/loss. Colors represent different models.

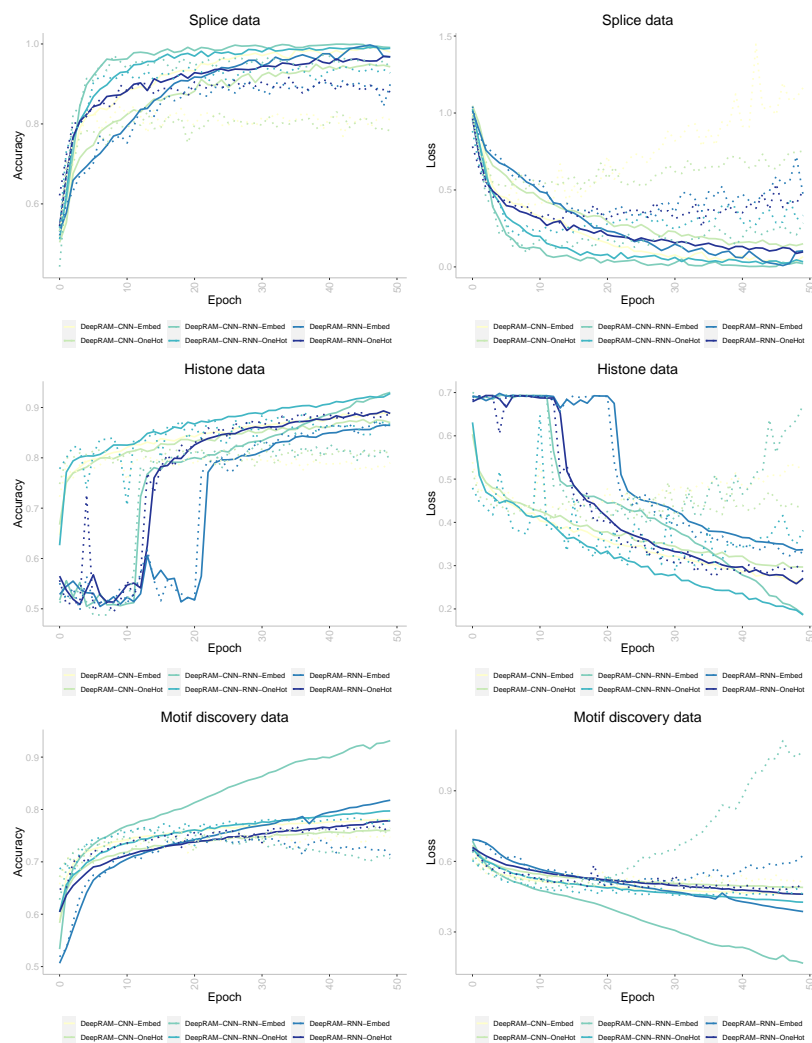


Figure 33: Learning dynamics for DeepRAM models on different datasets and different data embedding. Solid lines correspond to training accuracy/loss and dashed lines correspond to validating accuracy/loss. Colors represent different models and different data embedding.

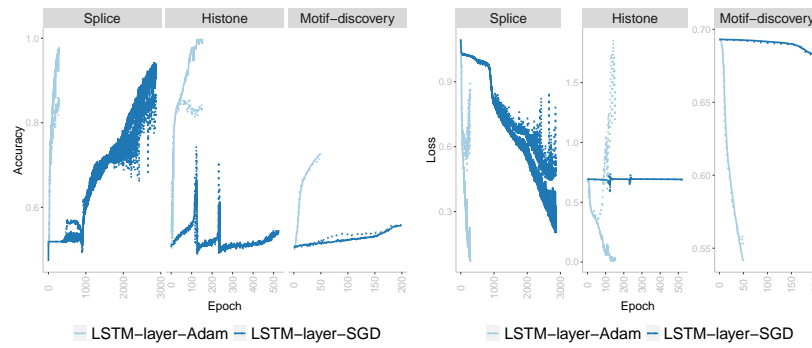


Figure 34: Learning dynamics for LSTM-layer model on different datasets and different optimizer. Solid lines correspond to training accuracy/loss and dashed lines correspond to validating accuracy/loss. Colors represent different optimizer.

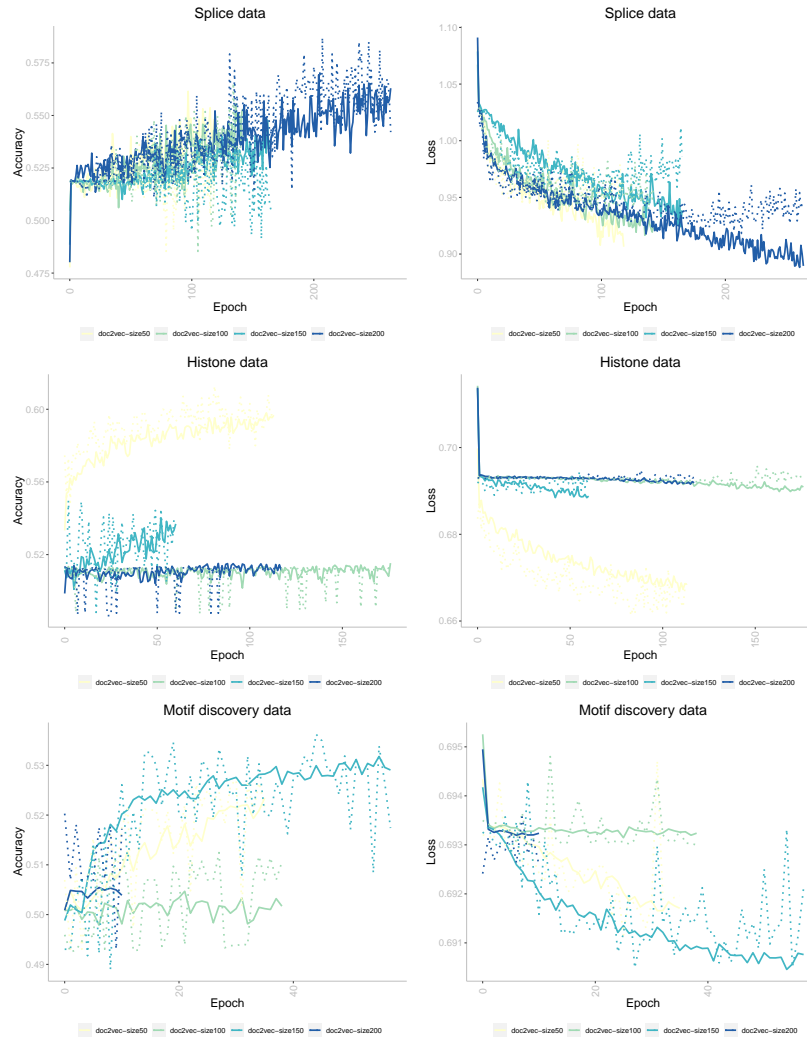


Figure 35: Learning dynamics for doc2vec+NN model on different datasets and different embedding sizes. Solid lines correspond to training accuracy/loss and dashed lines correspond to validating accuracy/loss. Colors represent different embedding sizes.

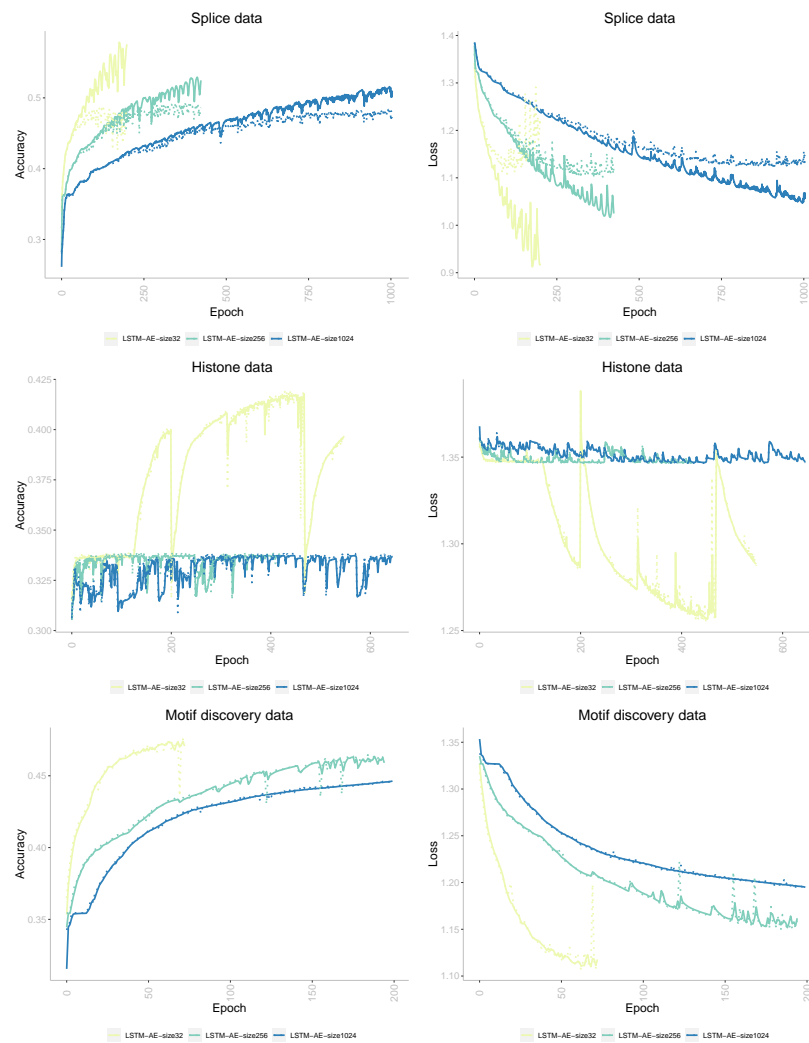


Figure 36: Learning dynamics for LSTM-AE+NN model on different datasets and different batch sizes. Solid lines correspond to training accuracy/loss and dashed lines correspond to validating accuracy/loss. Colors represent different batch sizes.

Table 4: Training details on NLP models. "Max. It." means maximum number of iterations allowed.

Model	Data	Max. It.	Patience	Early Stop	Optimizer
LSTM-AE (32)	Splice	2000	100	1474	Adam (LR=0.001)
LSTM-AE+NN (32)	Splice	1000	100	123	SGD (LR=0.01)
LSTM-AE (256)	Splice	2000	100	424	Adam (LR=0.001)
LSTM-AE+NN (256)	Splice	1000	100	114	SGD (LR=0.01)
LSTM-AE (1024)	Splice	2000	100	1005	Adam (LR=0.001)
LSTM-AE+NN (1024)	Splice	1000	100	200	SGD (LR=0.01)
LSTM-layer	Splice	4000	100	289	Adam (LR=0.001)
LSTM-layer	Splice	4000	100	2872	SGD (LR=0.01)
doc2vec+NN (50)	Splice	1000	50	119	SGD (LR=0.01)
doc2vec+NN (100)	Splice	1000	50	143	SGD (LR=0.01)
doc2vec+NN (150)	Splice	1000	50	166	SGD (LR=0.01)
doc2vec+NN (200)	Splice	1000	50	264	SGD (LR=0.01)
LSTM-AE (32)	Histone	4000	100	549	Adam (LR=0.001)
LSTM-AE+NN (32)	Histone	1000	100	212	SGD (LR=0.001)
LSTM-AE (256)	Histone	4000	200	422	Adam (LR=0.001)
LSTM-AE+NN (256)	Histone	1500	200	805	SGD (LR=0.001)
LSTM-AE (1024)	Histone	4000	200	646	Adam (LR=0.001)
LSTM-AE+NN (1024)	Histone	1500	200	999	SGD (LR=0.001)
LSTM-layer	Histone	3000	100	154	Adam (LR=0.001)
LSTM-layer	Histone	4000	400	526	SGD (LR=0.01)
doc2vec+NN (50)	Histone	1000	30	114	SGD (LR=0.01)
doc2vec+NN (100)	Histone	1000	30	177	SGD (LR=0.01)
doc2vec+NN (150)	Histone	1000	30	61	SGD (LR=0.01)
doc2vec+NN (200)	Histone	1000	30	118	SGD (LR=0.01)
LSTM-AE (32)	Motif	200	10	78	Adam (LR=0.001)
LSTM-AE+NN (32)	Motif	500	10	185	SGD (LR=0.01)
LSTM-AE (256)	Motif	200	10	195	Adam (LR=0.001)
LSTM-AE+NN (256)	Motif	500	10	146	SGD (LR=0.01)
LSTM-AE (1024)	Motif	200	10	200	Adam (LR=0.001)
LSTM-AE+NN (1024)	Motif	500	10	62	SGD (LR=0.01)
LSTM-layer	Motif	200	5	51	Adam (LR=0.001)
LSTM-layer	Motif	200	5	200	SGD (LR=0.01)
doc2vec+NN (50)	Motif	400	10	36	SGD (LR=0.01)
doc2vec+NN (100)	Motif	400	10	39	SGD (LR=0.01)
doc2vec+NN (150)	Motif	400	10	58	SGD (LR=0.01)
doc2vec+NN (200)	Motif	400	10	11	SGD (LR=0.01)

Table 5: Models with the highest testing accuracy for each dataset.

Model	Splice	Histone	Motif discovery
CNN-Nguyen	original (two 2D layer)	extra 1D layer	extra 1D layer
CNN-Zeng	four layers L2-reg	four layers L2-reg	four layers L2-reg
DeepRAM	RNN-Embed	RNN-OneHot	RNN-OneHot
LSTM-layer	SGD	ADAM	ADAM
LSTM-AE	batch size 1024	batch size 1024	batch size 1024
doc2vec	embed size 150	embed size 50	embed size 150